Computers and Chemical Engineering 134 (2020) 106675

Contents lists available at ScienceDirect

Computers and Chemical Engineering

journal homepage: www.elsevier.com/locate/compchemeng

# A Systematic Framework for the synthesis of operable process intensification systems – Reactive separation systems

Yuhe Tian[a,b], Iosif Pappas[a,b], Baris Burnak[a,b], Justin Katz[a,b], Efstratios N. Pistikopoulos[a,b,*]

[a] Artie McFerrin Department of Chemical Engineering, Texas A&M University, College Station, TX 77843, United States
[b] Texas A&M Energy Institute, Texas A&M University, College Station, TX 77843, United States

ARTICLE INFO

*Article history:*
Received 17 October 2019
Revised 28 November 2019
Accepted 4 December 2019
Available online 10 December 2019

*Keywords:*
Process intensification
Process synthesis
Process operability
Inherent safety
Explicit model predictive control
Reactive separation

ABSTRACT

In this work, we propose a systematic framework to synthesize process intensification systems with guaranteed operability, safety, and control performances accounting for both steady-state design and dynamic operation. A step-wise procedure is outlined which synergizes: (i) phenomena-based process synthesis with the Generalized Modular Representation Framework to derive novel intensified design configurations, (ii) flexibility and risk analysis for evaluation of operability and inherent safety performances at conceptual design stage, (iii) explicit/multi-parametric model predictive control following the PAROC (PARametric Optimisation and Control) framework to ensure dynamic operation under uncertainty, and (iv) simultaneous design and control via dynamic optimization to close the loop for the design of verifiable, operable, and optimal intensified systems. The proposed framework is demonstrated through a reactive separation case study for methyl tert-butyl ether production. Multiple process solutions are generated to showcase the trade-offs between economic and operational performances.



## 1. Introduction

Today's chemical process industry is faced with pressing challenges to sustain the increasingly competitive global market with rising concerns on energy, water, food, and environment (U.S. Energy Information Administration, 2019; International Energy Agency, 2018; BP plc, 2019; Intergovernmental Panel on Climate Change, 2014). Process intensification (PI) offers many promising opportunities to address these challenges by realizing step changes in process economics, energy efficiency, and environmental impacts through the development of novel process schemes and equipment (Stankiewicz and Moulijn, 2000; Tian and Pistikopoulos, 2019b; Bielenberg and Palou-Rivera, 2019; Tula et al., 2019). Intensified process solutions have also been well-recognized to synergize the advances in energy systems (Demirhan et al., 2019), smart manufacturing (Baldea et al., 2017), sustainable development (Charpentier, 2007), and circular economy (Avraamidou et al., 2020).

In this context, PI has gained significant impetus in the past decades featuring both successful industrial applications and burgeoning scientific research interests, which has been extensively reviewed in Keil (2018) and Tian et al. (2018a). Despite these progresses, PI is mostly regarded as an Edisonian effort driven by breakthrough engineering thinking while lack of theory and rigorous understanding (Baldea et al., 2019). Therefore, efforts have been made from the process systems engineering (PSE) perspective to provide more systematic approaches for the design and operation of process intensified systems (Tian et al., 2018a). A number of comprehensive review papers have highlighted the challenges for model-based computer-aided synthesis, design, optimization, and operational analysis of PI systems (Moulijn et al., 2006; Lutze et al., 2010; Babi et al., 2016; Tian et al., 2018a; Burnak et al., 2019). More recently, several special issues have been edited with specific interest in process intensification through process systems engineering, providing state-of-the-art perspective/review articles along with research contributions in this field (Wilhite and Ierapetritou, 2019; Bielenberg et al., 2018; Baldea et al., 2019).

Synthesis and design of PI systems are the key to drive for "innovation" of process systems. To enrich the design space with "out-of-the-box" novel process solutions, a promising trend in the PSE community is to generate chemical processes using phenomena-based representation (e.g., reaction, separation, mixing, heating) instead of conventional unit operation concept (e.g., reactor, distillation, heat exchanger) (Tian and Pistikopoulos, 2019b; Demirel et al., 2019b; Sitter et al., 2019). Synthesizing from the phenomena level offers the following advantages: (i) to discover novel process alternatives without any pre-postulation of plausible equipment and/or flowsheet configurations, (ii) to exploit the synergy between

* Corresponding author.
*E-mail address:* stratos@tamu.edu (E.N. Pistikopoulos).

https://doi.org/10.1016/j.compchemeng.2019.106675
0098-1354/

**Table 1**
Phenomena-based synthesis frameworks for process intensification - an indicative list.

| Author | Synthesis approach | Building block | PI Application | Key feature |
|---|---|---|---|---|
| Pistikopoulos & co-workers (Papalexandri and Pistikopoulos, 1996; Proios and Pistikopoulos, 2006; Tian and Pistikopoulos, 2018; 2019a) | Generalized Modular Representation Framework (GMF) | Pure heat exchange module & Mass/heat exchange module | Reactive separation, Extractive separation, Heat-integrated/ thermally-coupled separation | Gibbs free energy-based driving force constraintsSuperstructure optimization |
| Sundmacher & co-workers (Freund and Sundmacher, 2008; Kaiser et al., 2016; 2018; Liesche et al., 2019) | FluxMax approach (FMA) | Heat & Mass flux | Reactor network, Heat-integrated reactor-separator-recycle | Flux optimization, Simultaneous synthesis & heat integration |
| Gani & co-workers (Lutze et al., 2013; Babi et al., 2015; Tula et al., 2017; Garg et al., 2019) | Sustainable process synthesis-intensification framework | Phenomena building block (PBB) | Bio-based chemical production, Hybrid separation, reactive separation | Computer-aided software tool (ProCAFD), Hybrid approach w/ stepwise procedure given a base design |
| Skiborowski & co-workers (Kuhlmann and Skiborowski, 2017; Kuhlmann et al., 2017) | Optimization-based approach toprocess synthesis | Reactor-Network-PBB(RN)-PBB | Reaction-separation systems | State-space representation |
| Hasan & co-workers (Demirel et al., 2017; Li et al., 2018b; 2018a; Demirel et al., 2019a) | Abstract building block | Phenomenological building block | Reactive separation, hybrid separation, Heat-/Work-integration | 2-D representation, Superstructure optimization |
| Manousiouthakis & co-workers (Burri et al., 2002; Zhou and Manousiouthakis, 2006; Pichardo and Manousiouthakis, 2017; da Cruz and Manousiouthakis, 2019) | Infinite-DimEnsionAl state-space (IDEAS) framework | Process operators & Distribution network | Reactor network, Reactive distillation | State-space representation, Infinite Linear Programming |

multifunctional phenomena (e.g., combined reactive/separation), (iii) to de-bottleneck process performance by intensifying fundamental chemical phenomena (e.g., chemical/physical equilibrium, mass transfer), and (iv) to achieve breakthrough process improvements by re-inventing existing unit operations. An indicative list of these approaches and their key features are presented in Table 1. However, one of the major challenges to phenomena-based synthesis/representation lies in the resulting combinatorial design space with possibly excessive computational load, which necessitates the effective incorporation of "driving force" concepts (Lopez-Arenas et al., 2019; Tian and Pistikopoulos, 2018) or "ultimate" thermodynamic/kinetic boundaries (Feinberg and Ellison, 2001; Frumkin and Doherty, 2018). Another yet open issue is how to extend the phenomena-based representation capabilities from conventional reaction/separation systems (e.g., distillation, membrane) to capture more diverse PI technologies, such as periodic systems (e.g., pressure swing adsorption), micro-scale systems (e.g., microreactor), and rotating systems (e.g., rotating packed bed).

To ensure the normal "operation" of derived intensified systems in practical implementation, operability, safety, control performances need to be assessed at the early design stage. The unique and formidable operational challenges posed by intensified structures have been extensively discussed in the open literature (Tian et al., 2018a; Dias and Ierapetritou, 2019), which includes: (i) loss of degrees of freedom due to tight integration (Baldea, 2015), (ii) reduced operating window due to shared operating parameters of multi-phenomena (e.g., reaction and separation) (Kiss et al., 2018), (iii) complex and nonlinear dynamic behaviour which necessitates advanced model-based control strategies (Nikačević et al., 2012), and (iv) safety concerns due to unfamiliar or extreme operating conditions (Etchells, 2005). An indicative list of operability/safety/control studies on intensified systems are provided in Table 2. As can be seen, in addition to merely evaluating the operability/safety/control performance in intensified systems, there have been increasing efforts to integrate these operability metrics with synthesis/optimization to systematically derive optimal designs with guaranteed operational performance. For example, Tian and Pistikopoulos, 2018 incorporates steady-state flexibility and safety considerations with phenomena-based GMF synthesis resulting in a single mixed-integer nonlinear programming formulation to deliver intensified structures with desired level of flexibility and inherent safety. Also leveraging phenomena-based PI design, Castillo-Landero et al. (2018) proposed a stepwise intensification methodology to minimize the number of equipment integrating economic, sustainability, and inherent safety assessments. As for dynamic operation, integrated design and control approaches have attracted considerable attention over the past years (Yuan et al., 2012; Diangelakis, Burnak, Katz, Pistikopoulos, 2017). Panjwani et al. (2005) has shown that design and control optimization can lead to more economically beneficial and better controlled reactive distillation systems than a sequential approach. Despite these efforts, key open question remains on how to define and incorporate effective and consistent operability, safety, and control metrics at different levels of PI design, spanning from phenomena-based synthesis, steady-state design, and dynamic operational optimization.

To summarize the major gaps identified for the synthesis and operation of PI systems:

- **Lack of PI synthesis representation approaches** – to efficiently screen the large design space and to systematically derive intensified designs
- **Lack of operability, safety, and control assessment metrics** – to evaluate control, operability, and safety aspects of PI units
- **Lack of a generally accepted methodology and/or 'protocol'** – to integrate PI synthesis, operability, safety, and control to ensure the operability and optimality of the derived intensified structures while delivering their expected functionality
- **Lack of commercial software [or even a software prototype]** – to fully support systematic PI with operability, safety, and control

In this work, we present a systematic framework to synthesize intensified process systems with guaranteed operability, safety, and control performances. It follows an integrated procedure to synergize state-of-the-art PI/PSE methods, including phenomena-based synthesis representation, flexibility analysis, inherent safety analysis, explicit/multi-parametric model predictive control via the PAROC framework, mixed-integer nonlinear optimization, as well as mixed-integer dynamic optimization. The proposed framework will: (i) provide a holistic approach to deliver verifiable and operable PI systems which systematically and consistently addresses steady-state and dynamic design and operation in intensified processes; (ii) derive optimal process solutions via the use of optimization-based design and operational strategies; (iii) generate multiple process solutions with desired level of operability performance for decision making.

**Table 2**
Operability/Safety/Control studies on PI systems - an indicative list.

| Operational aspect | Author | PI application | Key feature |
|---|---|---|---|
| Flexibility | Pistikopoulos & co-workers (Tian and Pistikopoulos, 2018) | Reactive separation | Integrated flexibility & safety assessment w/ phenomena-based synthesis |
| | Chen and Westerberg (Chen and Westerberg, 1986; Westerberg and Chen, 1986) | Heat-integrated distillation | Analysis and synthesis with structural flexibility |
| Operability | Lima & co-workers (Gazzaneo and Lima, 2019; Carrasco and Lima, 2017) | Membrane reactor | Optimization-based operability approach for design, intensification & modularization |
| Control | Pistikopoulos & co-workers | Multicolumn CountercurrentSolvent Gradient Purification (Papathanasiou et al., 2019) | Explicit/Multi-parametric model predictive control |
| | | Pressure swing adsorption (Khajuria and Pistikopoulos, 2013) | Simultaneous design & control |
| | Gani & co-workers (Mansouri et al., 2016a; 2016b) | Reactive distillation | Integrated design and control |
| | Kiss & co-workers (Kiss and Rewagad, 2011; Rewagad and Kiss, 2012) | Dividing wall column | PID control, model predictive control |
| | Luyben & co-workers | Reactive distillation (Al-Arfaj and Luyben, 2002a; 2002b) | PID control |
| | | Extractive distillation (Luyben, 2008a; 2008b) | |
| | | Dividing wall column (Ling and Luyben, 2009a; 2009b) | |
| Safety | Pistikopoulos & co-workers (Tian et al., 2018c; 2018b) | Reactive separation, Heat-integrated systems | Risk assessment integrated w/ synthesis |
| | Jimenez-Gutierrez & co-workers | Extractive distillation (Medina-Herrera et al., 2014) | Consequence analysis w/ economic-safety multiobjective optimization |
| | | Reactive separation (Castillo-Landero et al., 2018) | Phenomena-based design w/ economic, sustainability & safety considerations |

The remaining of the paper is organized as follows: Section 2 formally states the synthesis problem considered in this work. In Section 3, we describe the proposed framework on a step-by-step basis, followed by a detailed introduction of involved synthesis and operability assessment methods. An extensive case study is presented in Section 4 to demonstrate the framework with application to a reactive separation process for methyl tert-butyl ether (MTBE) production. Concluding remarks on its application and future extension are discussed in Section 5.

## 2. Problem statement

The following problem definition presents the generalized problem addressed in this article for the synthesis of process intensification systems with operability, safety, and control considerations.

*Given:*

1. *Process design target*
   - A set of feed streams with given flowrate, composition, and supply temperature;
   - A set of desired products and specifications on their flowrates, temperatures, and/or purities;
   - A set of available heating/cooling utilities such as steam and cooling water with their availability, supply temperatures, and compositions;
   - A set of available mass utilities such as mass separating agents (e.g., entrainer, adsorbent) and catalysts;
   - All reaction schemes and kinetics data;
   - All physical property models;
   - Cost data of feeds, mass/heat utilities, and equipment;
2. *Flexibility target*
   - A specified range for uncertain parameters, where process flexibility is desired (e.g., feedstream composition, flowrate, and temperature, heat utility flowrate and temperature);
3. *Safety target*
   - A set of assessment criteria on inherent safety performances (e.g., toxicity, flammability, explosiveness);
   - A set of available equipment with their failure frequency data;
   - Hazardous property data (e.g., lethal concentration);
4. *Control target*
   - A set of disturbances during process operation;
   - A set of control variables with desired set-points;
   - A set of available manipulated variables to maintain feasible operation based on degrees of freedom analysis.

*Objective:*
To determine process solutions with

- Minimized total annualized cost consisting of capital cost, heat utility cost, and mass utility cost.
- Optimal equipment/flowsheet configuration(s) with design and operating parameters and satisfying desired flexibility and inherent safety criteria for both steady-state design and dynamic operation.
- Optimal control actions to achieve process specifications.

## 3. The framework for process synthesis-intensification with operability, safety, and control considerations

To address the above problem for the synthesis of operable process intensification systems, we propose a systematic framework as depicted in Fig. 1. In what follows, we first present the stepwise procedure to integrate steady-state synthesis, dynamic operational optimization, and operability assessment for delivery of verifiable and operable intensification designs. The specific synthesis and analysis techniques, which lay the basis to achieve this purpose, are then introduced in detail, i.e. Generalized Modular Representation Framework, Flexibility test, Risk assessment, and the PAROC (PARametric Optimisation and Control) Framework.

### 3.1. Overview of the proposed framework

*Step 1: Process Intensification/Synthesis Representation*

The first step is to represent chemical processes via the Generalized Modular Representation framework (GMF) (Ismail et al., 2001; Papalexandri and Pistikopoulos, 1996; Proios and Pistikopoulos, 2006; Tian and Pistikopoulos, 2018) from phenomena level without any pre-postulation of possible unit-operation-based process alternatives which may hinder the discovery of novel intensified process solutions. Two types of modular building blocks – i.e.

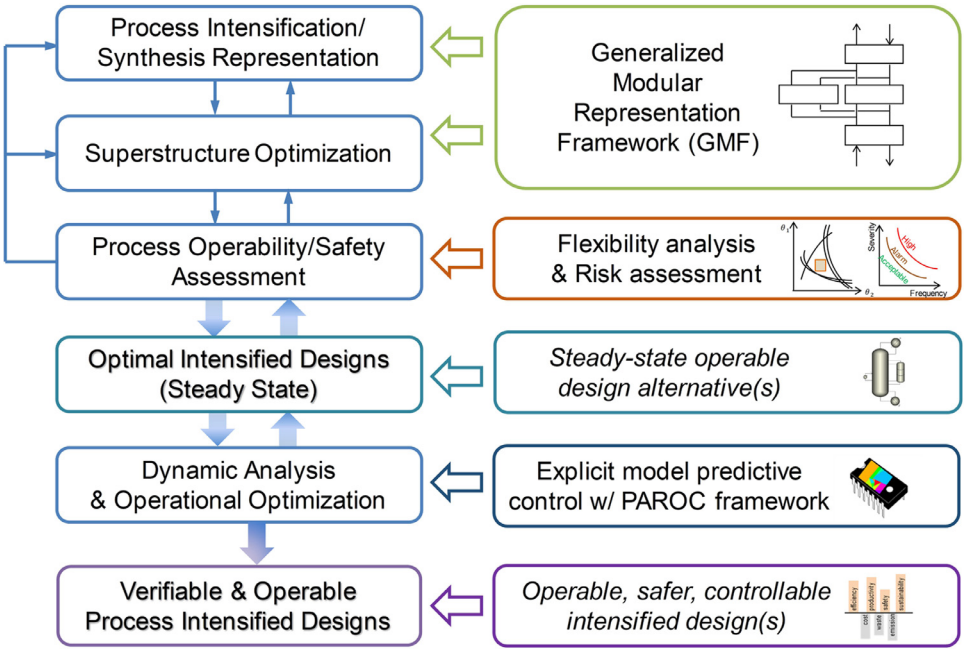


**Fig. 1.** The proposed framework for synthesis of operable PI systems.

pure heat exchange module and multifunctional mass/heat exchange module – are employed in GMF to overcome process bottlenecks by intensifying process fundamental performance, such as improving mass/heat transfer and/or shifting reaction equilibrium. Gibbs free energy based driving force constraints are derived to characterize mass transfer feasibility, thus providing a more compact and effective synthesis representation strategy exploiting the "ultimate" thermodynamic space. The detailed representation and mathematical basis of GMF will be presented later in Section 3.2.

*Step 2: Superstructure Optimization*

A superstructure formulation is developed based on GMF modular building blocks to account for all possible network configurations. The overall synthesis problem is formulated as a mixed-integer nonlinear programming (MINLP) problem which enables efficient screening of the resulting combinatorial design space (Ismail et al., 2001; Tian and Pistikopoulos, 2018). The solution of this optimization problem will identify the optimal GMF modular process alternatives with respect to a pre-defined objective function (e.g., total annualized cost, energy consumption, environmental impact). Alternative process solutions can also be generated by introducing integer cuts into synthesis model formulation (Floudas, 1995; Tian and Pistikopoulos, 2019a), since arguably even "intermediate" solutions can provide useful information on the process.

*Step 3: Steady-state Operability/Safety Assessment*

After obtaining the nominal optimal design[1] from Step 2 as base design, flexibility and safety metrics are introduced to assess steady-state operability performance of the derived intensified structure. In this work, flexibility test (Halemane and Grossmann, 1983; Grossmann and Floudas, 1987) (Section 3.3) is utilized to evaluate the functionality of resulting design under varying operating conditions, and risk assessment (Nemet et al., 2017; 2018) (Section 3.4) is applied to indicate its inherent safety performance by accounting for process consequence severity and equipment failure frequency. If the nominal design fails the operability and safety assessment, alternative design structures will be derived by incorporating flexibility and safety targets into GMF synthesis model to deliver GMF modular structures with guaranteed steady-state flexibility and safety performances without compromising process specifications (Tian and Pistikopoulos, 2018). However, the cost performance of the more operable and safer designs will be inferior than that of the nominal design due to the trade-offs on operability and safety. Note that other model-based operability criteria can also be incorporated, such as safety indices (Roy et al., 2016) and structural controllability (Lin, 1974), given that their required design and operation information for assessment are readily available at this phenomena-based design stage.

*Step 4: Optimal Intensified Steady-State Designs*

The resulting GMF modular designs with enhanced flexibility and safety performances will be translated to equipment-based process alternatives and will be validated using steady-state simulation tools. The identification of process equipment or flowsheet is mostly based on heuristics suggested by the types of GMF module, their interconnections, and operating conditions. For example, a mass/heat exchange module for (reactive) separation can be translated to either a column section for (reactive) distillation/absorption/etc., or a (reactive) membrane unit which satisfies the performance targets given by GMF synthesis results. Rigorous steady-state design is then performed to optimize the derived process units to determine optimal design and operating parameters.

*Step 5: Dynamic Analysis and Operational Optimization*

In this step, we take the above identified intensified process solutions to dynamic analysis. First, a high-fidelity dynamic model is developed to accurately describe the process dynamic behaviour which can be highly nonlinear with strong variable interactions in such intensified systems (Nikačević et al., 2012). To ensure that the desired operational performances have been succeeded from steady-state design, the dynamic systems are then analyzed with respect to flexibility and safety performance. After the consistency check, simultaneous design and control is performed to ensure economical and smooth operation despite the influence of disturbances. It is achieved by integrating the rigorous process model

[1] In this work, "nominal optimal design" refers to the optimal design obtained without operability/safety/control considerations.

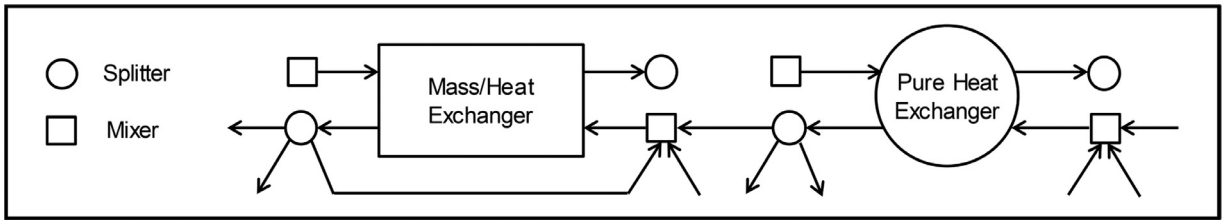


**Fig. 2.** GMF modular building blocks.

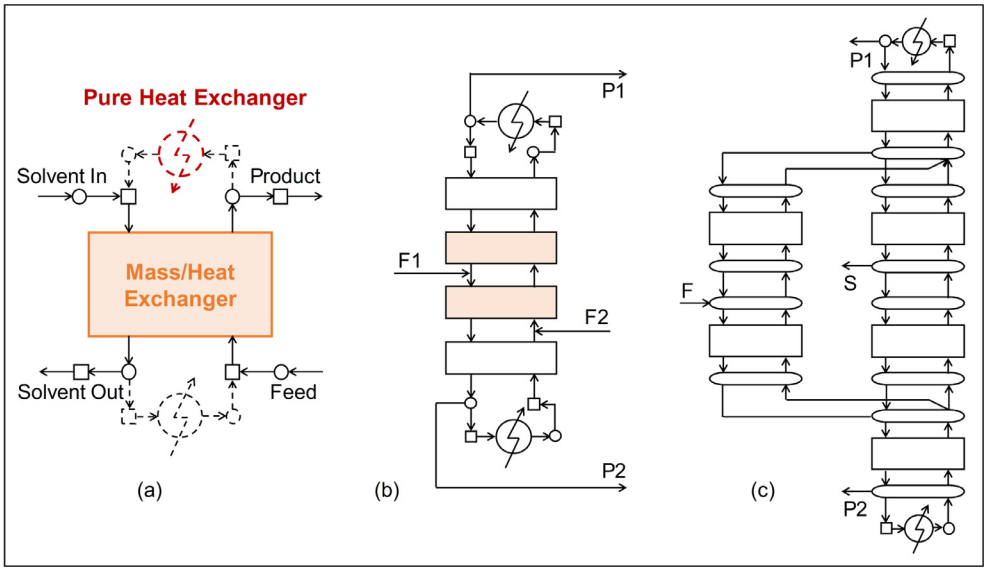


**Fig. 3.** GMF modular representation examples (a) Reactive absorption (Algusane et al., 2006), (b) Reactive separation (Ismail et al., 2001), (c) Petlyuk column (Proios and Pistikopoulos, 2006) Shaded M/H module: separation & reaction, Blank M/H module: pure separation.

and design dependent explicit controllers via mixed-integer dynamic optimization following the PAROC framework (Section 3.5).

*Step 6: Verifiable & Operable Process Intensification Designs*

The outcomes of this framework will be intensified process solutions with: (i) optimal process design and operating configurations (steady-state and dynamic validated); (ii) guaranteed operability and safety performances, and (iii) optimal explicit model predictive controller design.

### 3.2. Generalized Modular Representation Framework

A process operation can be generally characterized by a set of mass- and heat- transfer phenomena, concerning mainly the mass transfer of one component from one phase to another (e.g., distillation) or from one substance to another (e.g., reaction) due to the difference in their chemical potentials (Papalexandri and Pistikopoulos, 1996). Based on this concept, GMF utilizes a pure heat exchange module (He) and a mass/heat exchange module (M/H) as modular building blocks to represent chemical processes (conventional or intensified), as shown in Fig. 2. GMF has been successfully applied to synthesize a number of PI systems in our previous works, including: reactive distillation (Ismail et al., 2001; Tian and Pistikopoulos, 2018), reactive absorption (Algusane et al., 2006), extractive separation (Ismail et al., 1999a; Tian and Pistikopoulos, 2019a), dividing wall column (Proios and Pistikopoulos, 2006), and heat-integrated distillation (Proios et al., 2005) (Fig. 3). For brevity, we will not present the comprehensive model formulation which enables GMF synthesis, intensification, and integration capabilities, while interested readers are referred to the above works for more detail.

Some key features, which set GMF apart from other phenomena-based approaches, are listed below:

- **Gibbs free energy based driving force constraints to characterize generic mass transfer feasibility**

  Given a M/H exchange module with multicomponent liquid-vapor mixture, mass transfer can occur between two participating streams when the total Gibbs free energy ($nG$) is decreasing, i.e.

$$d(nG)^{tot}_{T,P} = dn_i \times \left[\frac{\partial (nG)^{tot}}{\partial (n_i)}\right]_{T,P} \leq 0 \tag{1}$$

  Eq. 1 is consistent with the following "driving force constraints" formulation:

$$G1_i \times G2_i \leq 0 \tag{2}$$

  where

$$G1_i = dn_i^L = f^{LO}x_i^{LO} - f^{LI}x_i^{LI} \tag{3}$$

$$G2_i = \left[\frac{\partial (nG)^{tot}}{\partial (n_i)}\right]_{T,P} = \ln\left[\frac{\gamma_i^L x_i^L P_i^{\mathrm{sat},L}}{\phi_i^V x_i^V P_{tot}}\right] + \sum_i \sum_k \left[\frac{\nu_{ik}\Delta G_i^f}{RT} + \nu_{ik}\ln\left(\phi_i^V x_i^V P_{tot}\right)\right]\frac{\partial \epsilon_k}{\partial n_i^L} \tag{4}$$

  In Eqs. 3 and 4, $i$ is the set of components, $n$ is the molar amount of substances, $L$ denotes liquid phase, $LO$ and $LI$ refer to respectively liquid outlet and inlet streams from or to the module, $f$ denotes flowrate, $x_i$ is for component molar fraction, $T$ and $P$ are respectively module temperature and pressure, $\gamma$ is activity coefficient, $\phi$ is fugacity coefficient, $P^{sat}$ represents

vapor saturated pressure, $\nu$ is stoichiometric coefficient, $\Delta G^f$ is the standard Gibbs function of formation.

The detailed derivation of $G2_i$ can be found in Tian and Pistikopoulos, 2018 using thermodynamic fundamental relationships such as Gibbs free energy expression for mixture, component mass conservation, and chemical potential expression.

- **Systematic identification of reaction and/or separation tasks from heat and/or mass transfer phenomena**
In the reactive distillation representation in Fig. 3b, a key question is how to dictate the identity of a mass/heat exchange module to perform pure separation task, pure reaction task, or hybrid reactive separation task. This is enabled by the above driving force constraints. As can be noted, $G2_i$ comprises two components:

  i separation component: $\ln\left[\frac{\gamma_i^L x_i^L P_i^{\text{sat},L}}{\phi_i^V x_i^V P_{tot}}\right]$

  ii reaction component: $\sum_i \sum_k \left[\frac{\nu_{ik}\Delta G_i^f}{RT} + \nu_{ik}\ln(\phi_i^V x_i^V P_{tot})\right]\frac{\partial \epsilon_k}{\partial n_i^L}$

Thus we introduce two sets of binary variables to denote the existence (or not) of separation and reaction phenomena in each M/H module, i.e. $y_{sep}$ and $y_{rxn}$. If $y_{sep} = 1$ then separation takes place; similarly $y_{rxn} = 1$ indicates the existence of reaction (otherwise the binary variables take the value of 0). If both $y_{sep} = 1$ and $y_{rxn} = 1$, the M/H module undertakes combined reaction/separation task.

Through the following big M constraints, reaction and/or separation phenomena can be systematically activated or deactivated in each M/H module without pre-postulation of reaction modules, separation modules, reactive separation modules, respectively:

$$-My_{sep} \le \ln\left[\frac{\gamma_i^L x_i^L P_i^{\text{sat},L}}{\phi_i^V x_i^V P_{tot}}\right] \le My_{sep}$$

$$-My_{rxn} \le \sum_i \sum_k \left[\frac{\nu_{ik}\Delta G_i^f}{RT} + \nu_{ik}\ln\left(\phi_i^V x_i^V P_{tot}\right)\right]\frac{\partial \epsilon_k}{\partial n_i^L} \le My_{rxn} \quad (5)$$

where $M$ is a (large) positive number.

- **Automated characterization of equilibrium and non-equilibrium tasks**
Note that the driving force constraints are derived based on $d(nG)^{tot}_{T,P} \le 0$ for feasible mass transfer, rather than $d(nG)^{tot}_{T,P} = 0$ for equilibrium state. That is, no physical or chemical equilibrium is enforced in GMF synthesis representation. Thus equilibrium-limited tasks ($G1_i \times G2_i = 0$) or kinetic-controlled tasks ($G1_i \times G2_i < 0$) will be identified as per process inherent characteristics or as per optimization results.

- **Enabling selection of functional materials within process tasks**
Material selection is achieved in GMF by utilizing rigorous thermodynamic models (e.g., NRTL, Redlich-Kwong-Soave equation) for calculation of phase equilibrium parameters (e.g., liquid activity coefficient $\gamma_i$, vapor fugacity coefficient $\phi_i$) to describe the nonideal mixture properties, as well as by incorporating rigorous reaction kinetics expression (e.g., reaction rate $r_k$) to capture the impact of catalysts.

GMF also supports inverse design, in which case a desired range of phase equilibrium parameters and/or kinetic parameters can be determined via optimization of process performance. The availability of desired material is then checked with available database (Tula et al., 2017) or synthesized via molecular design (Kalakul et al., 2018). While reactive separation with determined reaction scheme is of focus in the current work, readers are referred to Ismail et al. (1999a) and Tian and Pistikopoulos (2019a) for GMF application in extractive separation systems with solvent selection.

- **Compact/Aggregated representation to avoid combinatorial explosion**
As shown in Fig. 3, another key question is what dictates the number of mass/heat exchange modules necessitated for each system representation. Actually, each M/H module is characterized by a certain mass transfer pattern (e.g., component A transfer from liquid phase to vapor phase, while components B and C from vapor to liquid), as implied by the driving force constraints (Ismail et al., 2001):

If component A is transferred from liquid phase to vapor phase, or is consumed by liquid phase reaction, the number of moles of component A in the liquid streams of the M/H module is decreasing, i.e.

$$G1_A = f^{LO}x_A^{LO} - f^{LI}x_A^{LI} \le 0 \quad (6)$$

The driving force constraints require $G1_A \times G2_A \le 0$. Therefore, as a function of module temperature, pressure, and compositions – which are optimization variables to be determined – $G2_A$ should satisfy

$$G2_A = \ln\left[\frac{\gamma_A^L x_A^L P_A^{\text{sat},L}}{\phi_A^V x_A^V P_{tot}}\right] + \sum_A \sum_k \left[\frac{\nu_{Ak}\Delta G_A^f}{RT} + \nu_{Ak}\ln\left(\phi_A^V x_A^V P_{tot}\right)\right]\frac{\partial \epsilon_k}{\partial n_A^L} \ge 0 \quad (7)$$

Similarly, if A is transferred from vapor phase to liquid phase, or is produced by liquid phase reaction,

$$G1_A = f^{LO}x_A^{LO} - f^{LI}x_A^{LI} \ge 0 \quad (8)$$

$$G2_A = \ln\left[\frac{\gamma_A^L x_A^L P_A^{\text{sat},L}}{\phi_A^V x_A^V P_{tot}}\right] + \sum_A \sum_k \left[\frac{\nu_{Ak}\Delta G_A^f}{RT} + \nu_{Ak}\ln\left(\phi_A^V x_A^V P_{tot}\right)\right]\frac{\partial \epsilon_k}{\partial n_A^L} \le 0 \quad (9)$$

In this context, taking distillation column representation as an example, each M/H module identifies an aggregation of columns trays, or in other words a column section (i.e. portion of a column not interrupted by entering or exiting streams or heat flows) (Proios, 2004). On the other hand, due to this aggregated representation capability benefited from Gibbs free energy based driving force constraints, the GMF synthesis/optimization problem is also in more compact size avoiding combinatorial explosion.

### 3.3. Flexibility analysis

Flexibility refers to the capability of a process to satisfy all relevant constraints under uncertain operating conditions, e.g. variations in product demand, quality targets, material properties, environmental conditions, etc. (Halemane and Grossmann, 1983; Grossmann and Floudas, 1987; Bhosekar and Ierapetritou, 2018; Tian et al., 2018a). As shown in Halemane and Grossmann (1983), a process synthesis problem with flexibility requirement $\forall V_\theta \in U(V_\theta)$ can be recast in the following compact mathematical form:

$$\max_{V_\theta \in U(V_\theta)} \min_{V_z} \max_{j \in J_f} \quad f_j(V_\theta, V_d, V_x, V_z) \le 0 \quad \text{s.t.} \quad h(V_\theta, V_d, V_x, V_z) = 0 \quad (10)$$

where $V_\theta$ is the set of uncertain parameters, $U(V_\theta)$ is the specified range of uncertainty; $V_d$ denotes the set of design variables; $V_x$ are

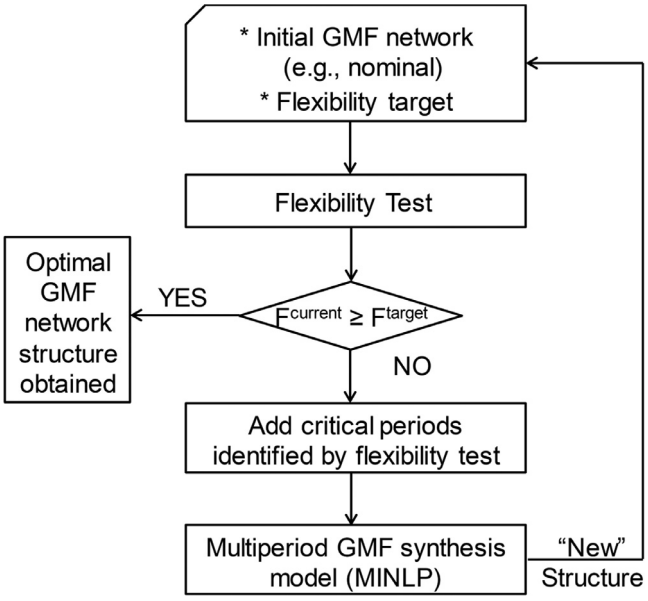


**Fig. 4.** Iterative scheme for flexibility analysis.

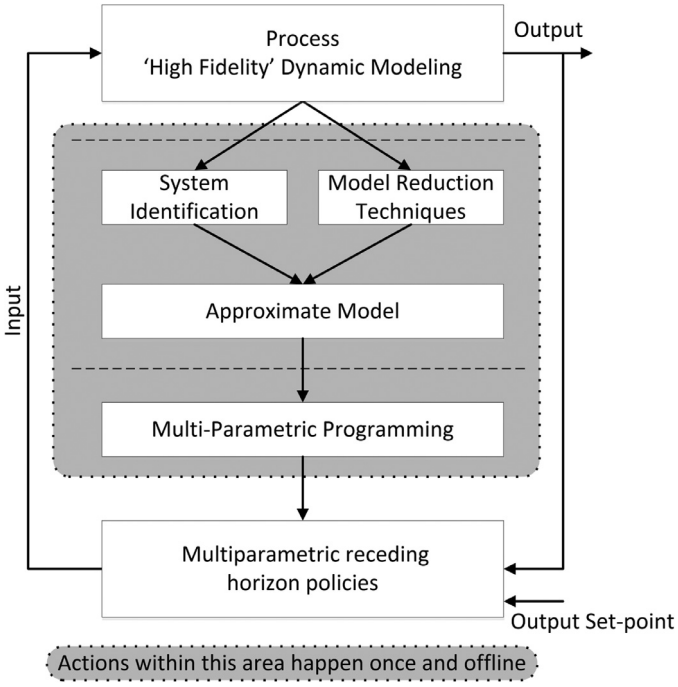


**Fig. 5.** The PAROC framework (adapted from Pistikopoulos et al. (2015)).

state variables; $V_z$ represents the set of manipulated variables that can be adjusted during operation; $f$ is the set of inequality model constraints; $J_f$ is the index set for the inequality constraints; and $h$ is the set of equality model constraints.

To avoid the direct solution of this tri-level optimization problem, an iterative discretization scheme has been developed by Papalexandri and Pistikopoulos (1994) for flexibility analysis of GMF networks. As illustrated in Fig. 4 (Tian and Pistikopoulos, 2018), the optimal GMF network structure obtained at nominal operation condition undergoes flexibility test (Halemane and Grossmann, 1983) to identify critical operating conditions which violate the desired nominal operating points in presence of uncertain parameters. Then via a multiperiod formulation, the identified critical operating conditions are incorporated in GMF superstructure representation as an additional set of operation "periods". Specifically, uncertain parameters $V_\theta$ (e.g., feed stream flowrates), state variables $V_x$ (e.g., stream temperatures, compositions), and manipulated variables $V_z$ (e.g., heat exhanger duties) are reformulated as variables for each period of operation "$s$", i.e. $V_{\theta,s}$, $V_{x,s}$, and $V_{z,s}$. However, design variables $V_d$ (e.g., diameter and height of mass exchange module) remain valid for all periods of operation. In this way, the resulting multiperiod GMF synthesis model will enable automated generation of optimal modular structure with guaranteed flexibility performance under uncertainty.

### 3.4. Risk assessment

Process risk can be used to evaluate the inherent safety performance of a chemical process by considering equipment failure frequency and consequence severity (Eq. 11), which can be readily incorporated into steady-state/dynamic model-based design and optimization for simultaneous process synthesis with inherent safety considerations (Nemet et al., 2017; 2018).

$$Risk = Failure\ Frequency \times Consequence\ Severity \tag{11}$$

Equipment failure frequency data can be taken from specific database such as that provided in the *Handbook of Failure Frequencies* (Flemish Government, 2009) or in the *Guideline for Quantitative Risk Assessment* (Stoffen, 2005). These average historical data are applicable for chemical unit operations (e.g., distillation column, reactor), which can be directly used in risk analysis with equipment-based flowsheet. However, for risk analysis at an earlier phenomenological design stage, the GMF pure heat exchanges modules and mass/heat exchange modules are approximated respectively as heat exchangers, process vessels (or reactor vessels depending on if reaction is taking place) (Tian and Pistikopoulos, 2018). The consistency of risk assessment between phenomena-based synthesis, steady-state equipment-based design, and dynamic operational optimization will be cross-validated throughout the framework implementation (Section 3.1).

Consequence severity is indicated by the indication number which measures the intrinsic hazard of a unit depending on the amount of substance present, the physical and toxic properties of the substance, and the specific process conditions (Freeman, 1989). The indication number, $A$, is a dimensionless number defined by Eq. 12:

$$A = \frac{W \times O^1 \times O^2 \times O^3}{S} \tag{12}$$

where $W$ denotes the mass quantity of hazardous substance existing in the process, $S$ is the limit value which measures the hazardous properties of each substance based on their physical properties and toxic/explosive/flammable properties, $O^i$ are the factors for process conditions, including: $O^1$ accounting for process unit versus storage unit, $O^2$ accounting for the positioning of the unit, and $O^3$ accounting for the amount of substance in the vapour phase after release.

### 3.5. The PAROC framework

The PAROC framework, standing for "PARametric Optimisation and Control", is a unified framework and software platform[2] for the design, operational optimization, and explicit/multi-parametric model-based predictive control (mp-MPC) of process systems (Pistikopoulos et al., 2015). As shown in Fig. 5, adapting this model-based control and optimization procedure offers the fol-

[2] The PAROC platform can be accessed via http://paroc.tamu.edu/.

lowing advantages for design and operational analysis of chemical process systems:

- **High fidelity modeling and analysis**
  The high fidelity dynamic model developed based on first-principles (e.g., mass and energy balances) are critical to the accuracy of process dynamic behavior and the validity of operational analysis. It normally consists of (Partial) Differential-Algebraic Equations, with continuous and binary design and operating variables which can be manipulated or optimized via later control and optimization steps. This modeling task takes place in PSE's gPROMS® ModelBuilder platform.

- **Exact MPC solution obtained via offline multi-parametric programming**
  Based on a linear approximated state-space model of the original high fidelity model, the MPC controller design problem is given by Eq. 13:

$$\begin{aligned}\min_{u}\quad & J = x_N^T P x_N + \sum_{k=1}^{OH-1}\left(\left(y_k - y_k^R\right)^T QR_k\left(y_k - y_k^R\right)\right) \\ & + \sum_{k=0}^{CH-1}\left(\left(u_{c,k} - u_{c,k}^R\right)^T R_k\left(u_{c,k} - u_{c,k}^R\right)\right) \\ \text{s.t.}\quad & x_{k+1} = Ax_k + Bu_{c,k} + C[d_k, De]^T \\ & y_k = Dx_k + Eu_{c,k} + e \\ & u_{min} \le u_{c,k} \le u_{max} \\ & \Delta u_{min} \le \Delta u_{c,k} \le \Delta u_{max} \\ & x_{min} \le x_k \le x_{max} \\ & y_{min} \le y_{c,k} \le y_{max}\end{aligned} \tag{13}$$

  where $x_k$ are the state variables, $u_{c,k}$ and $u_{c,k}^R$ are the control variables and their set points, $y_k$ and $y_k^R$ are the output variables and their set points, $d_k$ denotes disturbance, $De$ gives the design variable, $QR_k$ and $R_k$ are respectively weight parameters for the MPC controller, $P$ is the stabilizing term derived from the Riccatti Equation for discrete systems, $OH$ and $CH$ are respectively the output horizon and control horizon, $k$ is the time step, $A, B, C, D, E$ are the matrices of the approximated linear state-space model, and $e$ gives the mismatch between the actual system output and the predicted output at initial time.

  Eq. (13) can be reformulated as a multiparametric programming problem (Bemporad et al., 2002), the solution of which via POP® toolbox (Oberdieck et al., 2016) in MATLAB® will give the explicit control actions as an affine function of systems variables (Eq. (14)) (Oberdieck et al., 2016):

$$\begin{aligned}u_{c,T} &= K_i\theta_T + r_i,\ \forall\theta_T \in CR_i \\ \theta_T &= \left[x_T; u_{c,T-1}; d_T; De; y_T; y_T^{SP}\right]\end{aligned} \tag{14}$$

  where $u_{c,T}$ denotes control variable, $\theta_T$ is the set of uncertain parameters in multi-parametric programming, $x_T, d_T, y_T, y_T^{SP}$ denote respectively the states, disturbances, outputs, and output setpoints, $u_{c,T-1}$ represents the optimal control action at the previous time step and $De$ is the design variable.

- **Design-dependent mp-MPC controller derivation**
  As can be noted in Eq. 14, design variable $De$ is treated as uncertain parameter and is aware by the optimal mp-MPC controller. Thus the derived design dependent mp-MPC controller can be applied for different design alternatives without a reformulation of the control problem for different design alternatives (Diangelakis et al., 2017).

- **Dynamic optimization for simultaneous design and control**
  By integrating the high-fidelity process model and mp-MPC controller, the optimal design with optimal control actions can be derived leveraging the advanced (mixed-integer) dynamic optimization strategies provided by PSE's gPROMS® software platform (Diangelakis et al., 2017).

## 4. Case study: Reactive separation for MTBE production

Reactive separation is one of the major PI inventions which exploits the synergy between multiple processing tasks to overcome process bottlenecks and to achieve significant energy and cost savings over conventional reactor-separator-recycle counterparts (Harmsen, 2007). In the current work, we will extend the case study given in Tian and Pistikopoulos, 2018 on reactive separation for methyl tert-butyl ether (MTBE) production, where we have derived intensified designs with safety and operability considerations through steady-state synthesis (Steps 1–4 of the proposed framework). Herein, we take the previous steady-state operable and safer designs to dynamic operational optimization with operability, safety, and control (Steps 5–6). We also highlight the consistency throughout the framework to ensure delivery of verifiable and operable PI systems.

For clarity and continuity, in this section we will demonstrate the proposed framework step-by-step, including brief review on steady-state design to show how innovation can be achieved through synthesis intensification, while stressing dynamic extensions to close the loop for the synthesis of intensified, operable, safer, and controllable MTBE production systems.

### 4.1. Problem definition

MTBE can be produced by reacting isobutylene (IB4) and methanol (MeOH) in the liquid phase catalyzed by an ion-exchange resin (i.e., Amberlyst 15). The reaction scheme is shown in Eq. (15).

$$\text{MeOH} + \text{IB4} \rightleftharpoons \text{MTBE},\quad \Delta_r H^o_{298\text{K}} = -37.7\text{kJ/mol} \tag{15}$$

The intrinsic rate of MTBE production is adapted from Rehfinger and Hoffmann (1990):

$$r = k\left[\frac{a_{IB4}}{a_{MeOH}} - \frac{1}{K_a}\frac{a_{MTBE}}{a_{MeOH}^2}\right]\quad \text{kmol/(h}\cdot\text{kg catalyst)} \tag{16}$$

where $r$ is the molar reaction rate per unit mass of dry catalyst resin, $a$ is the activity of each component. The temperature-dependent expression for rate constant $k$ is given by Eq. (17) (Rehfinger and Hoffmann, 1990):

$$k = 8.5132\times 10^{13}\exp\left[\frac{-11113.78}{T}\right]\quad \text{kmol/(h}\cdot\text{kg catalyst)} \tag{17}$$

where $T$ is the process temperature in K. The expression of reaction equilibrium constant $K_a$ is determined via Eq. 18 adapted from Colombo et al. (1983):

$$\ln K_a = -10.0982 + \frac{4254.05}{T} + 0.2667\ln T \tag{18}$$

The liquid mixture of methanol, butene, and MTBE is highly nonideal. The UNIQUAC equations are utilized to calculate the liquid activity coefficients as suggested by Rehfinger and Hoffmann (1990). Saturated vapor pressures are calculated via the Antoine equation with the component-specific parameters provided by Ismail et al. (2001).

*Given:*

- Feed streams – as shown in Table 3, a feed stream of pure liquid methanol and a feed stream of saturated vapor butenes are available as raw materials. Note that an inert component 1-butene (NB4) also exists in the feed stream

**Table 3**
Feed conditions (nominal values).

| | Liquid feed | Vapor feed |
|---|---|---|
| Temperature (K) | 320 | 350 |
| Flowrate (mol/s) | 215.5 | 545 |
| $x_{MeOH}$ | 1 | 0 |
| $x_{IB4}$ | 0 | 0.3578 |
| $x_{NB4}$ | 0 | 0.6422 |
| $x_{MTBE}$ | 0 | 0 |
| Pressure (atm) | 11 | 11 |

**Table 4**
Hazardous property data.

| | $LC_{50}$ (rat,1h,inh)/mg | Flam | TNT equivalence/kg |
|---|---|---|---|
| MeOH | 65.6 | Yes | 4.62 |
| IB4 | 155 | Yes | 2.05 |
| NB4 | 164.5 | Yes | 2.03 |
| MTBE | 21.3 | Yes | 2.62 |

- Product specifications – the desired product is liquid MTBE with 98% purity at a flowrate of 197 mol/s
- Heating/Cooling utilities – steam and cooling water are available as utilities, respectively at the price of 137.27 US$/(kW · yr) and 26.19 US$/(kW · yr) (Ismail et al., 2001)
- Equipment cost data – this will be provided later depending on the identified process solutions via GMF synthesis
- Uncertainty in methanol feed flowrate – 215.5 ± 10 mol/s
- Toxicity, flammability, and explosiveness property data – the hazardous properties for each component are summarized in Table 4
- Disturbance in IB4 inlet composition – a randomly generated disturbance during operation with a range of 0.3578 ± 0.05

*Objective:*

Determine process solution(s) with the optimal economic performance with respect to total annualized cost (Eq. (19)) as well as with smooth and safe operation despite the influence of disturbances and uncertainty.

$$\text{Total Annualized Cost}(\$/\text{yr}) = Cost_{utilities} + \frac{Capital\,Cost}{Payback\,period} \quad (19)$$

### 4.2. Process intensification/synthesis representation with generalized modular representation framework

As introduced in Section 3.2, GMF mass/heat exchange (M/H) modules and pure heat exchange (He) modules (Fig. 2) are employed to represent this MTBE production process with underlying driving force constraints to characterize mass/heat transfer feasibility without any pre-postulation of process reaction/separation tasks or equipment/flowsheet configurations.

A maximum of 10 mass/heat exchange modules and 20 pure heat exchange modules are assigned to be available for initial use in representation and optimization. Once this bound is active, the value is relaxed to allow more modules to be used. However, it is a key yet open question how to determine an "optimal" set of available mass/heat exchange modules to well-balance representation accuracy and computational complexity. To obtain an estimate on the number of modules before proceeding with superstructure optimization, simulation studies can be performed to synthesize any reference MTBE production flowsheets available in open literature as detailed in Tian and Pistikopoulos, 2018. A combinatorial superstructure network, as shown in Fig. 6, is utilized to interconnect these GMF modules which can encompass any plausible process alternatives including both conventional and intensified configurations (Ismail et al., 1999b).

### 4.3. Superstructure optimization

The above GMF synthesis model is implemented in General Algebraic Modeling System (GAMS) and solved with Generalized Benders Decomposition (GBD) strategy. The GBD method is adapted herein because of the control it provides during the solution procedure, which is essential for this type of highly nonconvex

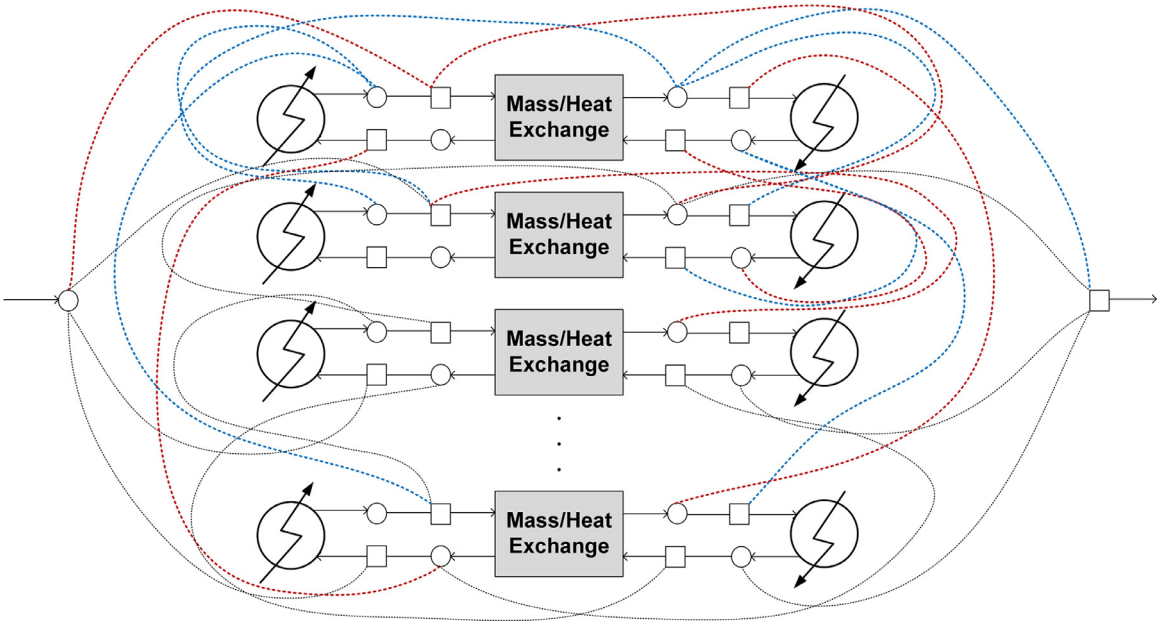


**Fig. 6.** GMF modular superstructure for process synthesis representation.
Red dashed lines: indicative interconnecting streams entering the 1st module.
Blue dashed lines: indicative interconnecting streams leaving the 1st module.
Grey dashed lines: indicative interconnecting streams between other modules.

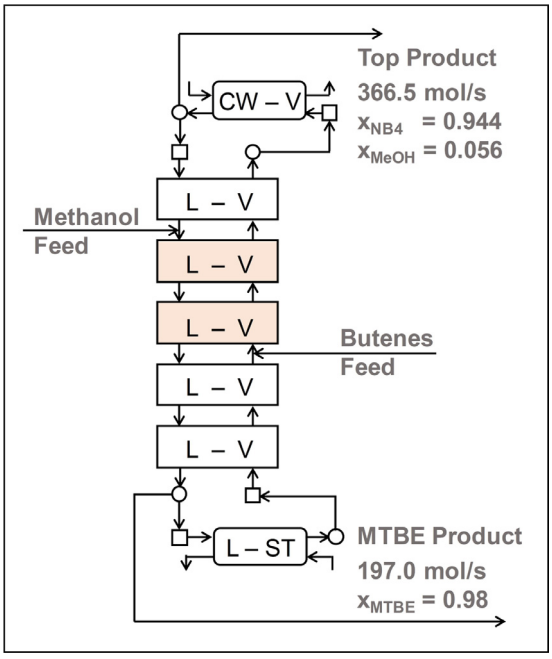


**Fig. 7.** Nominal GMF modular design for MTBE production.

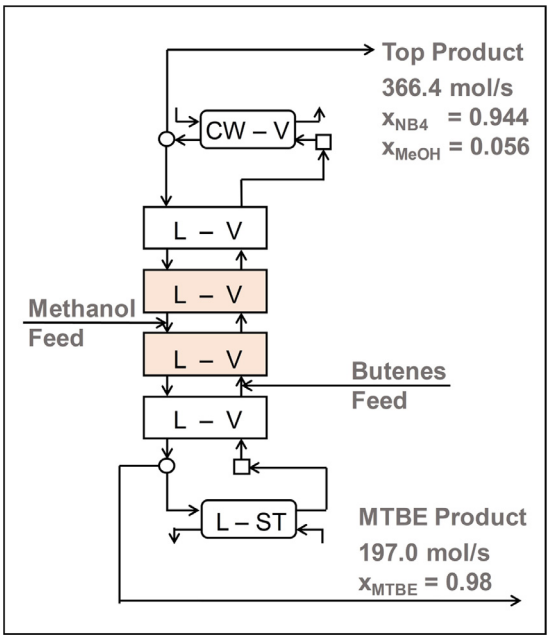


**Fig. 8.** Flexible & Inherently safer GMF modular designs for MTBE production: Operable Design 1.

MINLP problems to avoid the large infeasible portion of the design space. It has also been observed that symmetry modular structures can be repetitively identified during the iterative solution procedure due to the representation with identical GMF modules. The solution strategy can be improved to prevent these degenerate solutions by introducing symmetry-breaking sequencing rules (Margot, 2010) to GBD MIP subproblem, while this is beyond the scope of this work.

The resulting cost-optimal solution[3] (i.e., Nominal Design) is depicted in Fig. 7, with a total annual cost of 1.71 $\times$ $10^6$\$/*yr*. It consists of two pure heat exchange modules and five mass/heat exchange modules in the final modular flowsheet configuration, featuring the same reactive distillation type of configuration as shown in previous GMF studies (Ismail et al., 2001). Two M/H modules are identified as reactive zone to undertake reactive separation task to produce MTBE. Among the other three M/H modules for pure separation, two serve as stripping section to separate unreacted methanol and isobutylene back to reaction zone, and the other one as rectification section to transfer n-butene to distillate.

### 4.4. Steady-State operability/safety assessment

Considering the uncertain methanol feed flowrate in the range of 215.5 $\pm$ 10 mol/s, flexibility test based on the nominal GMF design shown in Fig. 7 identifies a critical point as $f^I_{MeOH} =$ 225.5 mol/s at which the system will deviate from the desired operating point. In this step, we aim to improve the flexibility performances of the derived structures to preserve nominal operating point under uncertainty, as well as to improve the inherent safety performance measured by reducing process risks.

*Operability & Safety Target 1*

To synthesize a cost-optimal GMF modular design which also satisfies the following operability and safety metrics:

- flexible in the presence of uncertainty in methanol feed flowrate (215.5 $\pm$ 10 mol/s)
- inherently safer than the nominal design by reducing at least 20% of process risk (respectively for toxicity risk, flammability risk, and explosiveness risk)

Following the integrated GMF-flexibility-safety synthesis strategy (Sections 3.3 and 3.4), the updated optimal process solution is illustrated in Fig. 8. Hereafter we will refer to this GMF design as "Operable Design 1". Comparing to the nominal design, flexibility requirement results in an increase of M/H module diameter in Operable Design 1 to accommodate feed flowrate uncertainty, while process risks are reduced in a more intuitive way by reducing the number of involved modules in the process. The total annual cost of Operable Design 1 is 1.82 $\times$ $10^6$\$/*yr*, featuring a 6.4% increase comparing with the Nominal Design.

However, it is noted that the second (numbered in a descending order) reactive separation module takes up more than 1/3 of the overall process risk, which renders it a comparatively more risky component in this flowsheet. To alleviate this effect, another enhanced operability and safety target is set as follows:

*Operability & Safety Target 2*

To synthesize a cost-optimal GMF modular design which also satisfies the following operability and safety metrics:

- flexible in the presence of uncertainty in methanol feed flowrate (215.5 $\pm$ 10 mol/s)
- inherently safer than the nominal design by reducing at least 20% of process risk (respectively for toxicity risk, flammability risk, and explosiveness risk)
- *risk of individual module is no more than 30% of the risk of overall process*

Incorporating the new model constraint to limit individual module risk gives rise to another optimal modular solution as shown in Fig. 9 (Operable Design 2). As can be noted, additional process streams are introduced to bypass the second reactive separation module which increases the system's degree of freedom

[3] A minimum value of 1.7 is set to the reflux ratio for realistic considerations of reactive distillation operation. Detailed discussion regarding intensification impacts on reflux ration is available in Tian and Pistikopoulos (2018).

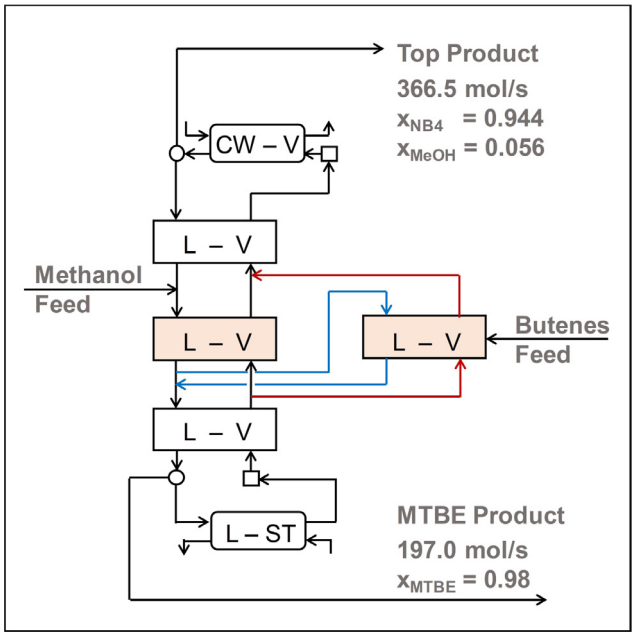


**Fig. 9.** Flexible & Inherently safer GMF modular designs for MTBE production: Operable Design 2.

as well as alleviates its mass/heat exchange burden for inherent safety concerns. The total annual cost of Operable Design 2 is $1.90 \times 10^6$\$/*yr*, featuring a 11.1% increase comparing with the Nominal Design.

Up to this step, we have generated three GMF modular design configurations with different cost performances and different level of operability and safety performances (Figs. 7–9). As can be noted, operability and safety considerations may result in significant structure changes of the process optimal configurations, illustrating the rigorous trade-off between process costs, operability, and safety.

### 4.5. Optimal intensified steady-state designs: Validation & simulation

In this step, we translate the resulting GMF modular structures to unit-operation-based process schemes and cross-validate phenomena-based synthesis results with steady-state rigorous simulation profiles. In what follows, we briefly present the identification and translation of GMF modular structures to equipment-based flowsheet alternatives as shown in Fig. 10. A detailed comparison of GMF synthesis results and corresponding Aspen validation results are summarized in Table 5.

#### *Nominal Design*

The GMF Nominal Design (Fig. 7) is translated into a reactive distillation column using RadFrac module in Aspen Plus®, assuming both physical and chemical equilibrium. Each GMF reactive separation module and the bottom separation module is translated to three column trays while the other separation modules to two column trays respectively, thus featuring a total of 15 stages (including reboiler and condenser). To determine the column's operating conditions using Aspen optimization analysis, column pressure and reflux ratio are manipulated to meet process specifications and to minimize operating cost as a function of condenser and reboiler heat duties.

#### *Operable Design 1*

Similarly, the GMF Operable Design 1 shown in Fig. 8 is translated to a reactive distillation column to the Nominal Design, with a total of 13 stages including reboiler and condenser.

#### *Operable Design 2*

The major part of the Operable Design 2 (Fig. 9), excluding the second reactive separation module, is translated to a main reactive distillation column. Additionally, the second reactive separation module is translated to a side column which is fully integrated

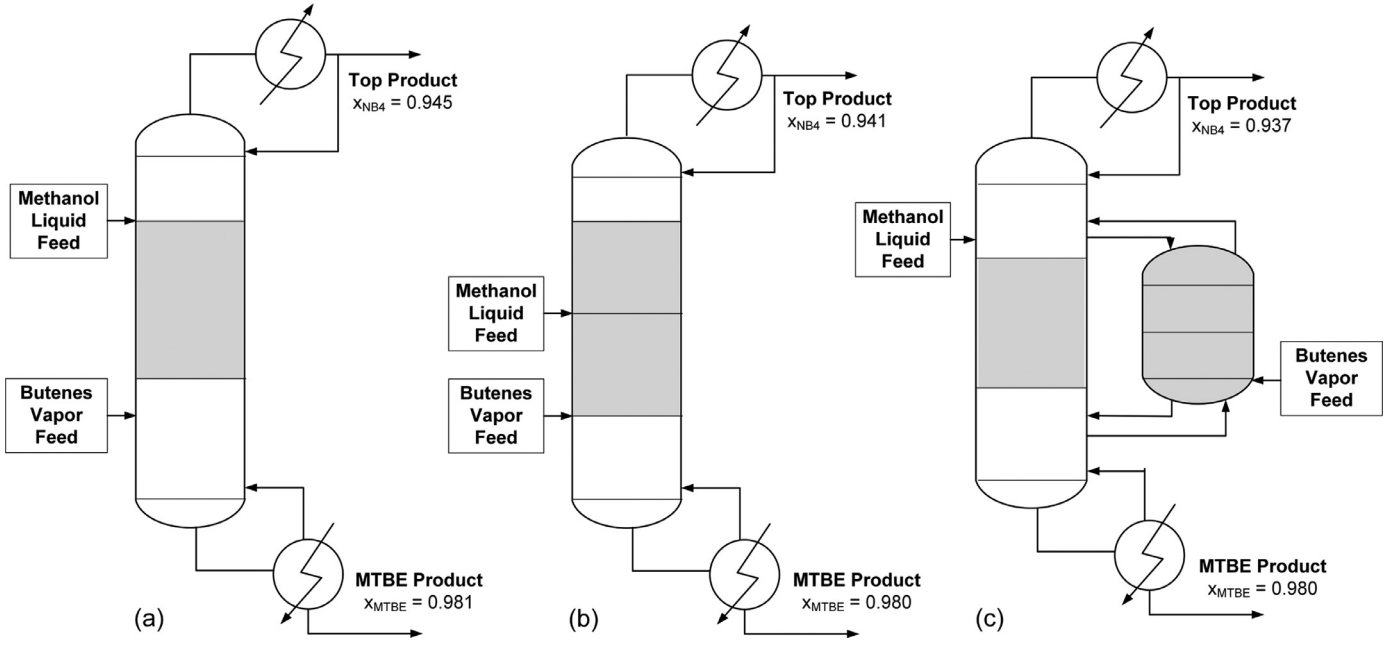


**Fig. 10.** Equipment-based flowsheet alternatives for MTBE production.
(a) Nominal Design, (b) Operable Design 1, (c) Operable Design 2.
Shaded trays: reactive zone.

**Table 5**
Quantitative comparison: GMF synthesis and Aspen validation.

| | Nominal design | | Operable design 1 | | Operable design 2 | |
|---|---|---|---|---|---|---|
| | GMF | Aspen | GMF | Aspen | GMF | Aspen |
| Column pressure (atm) | 5.46 | 6.00 | 7.85 | 7.95 | 9.48 | 8.20 |
| Reflux ratio | 1.70 | 2.10 | 1.70 | 2.50 | 1.70 | 3.30 |
| Reboiler duty (MW) | 7.5 | 6.6 | 8.4 | 9.6 | 8.9 | 20 |
| Condenser duty (MW) | 23 | 22 | 23 | 24 | 23 | 34 |
| Module/Tray Number | 7 | 15 | 6 | 13 | 6 | 10+3* |
| Product flowrate (mol/s) | 197.0 | 197.0 | 197.0 | 197.0 | 197.0 | 197.0 |
| Product purity (mol/mol) | 0.98 | 0.98 | 0.98 | 0.98 | 0.98 | 0.98 |

* Main column: 10 trays, Side column: 3 trays.

**Table 6**
Design & Operation parameters for dynamic simulation.

| | Nominal design | Operable design 1 | Operable design 2 |
|---|---|---|---|
| Number of stages | 17 | 15 | 11 (main)<br>3 (side) |
| Reactive stages | 4–11 | 4–11 | 2–6 (main)<br>1–3 (side) |
| Pressure (atm) | 6 | 7.9 | 8.2 |
| Reflux ratio | 2.11 | 2.75 | 4 |
| Reboiler duty (MW) | 6.84 | 11.4 | 20.0 |
| Condenser duty (MW) | 21.8 | 25.4 | 33.9 |
| Product purity (mol/mol) | 0.98 | 0.98 | 0.98 |
| Product flowrate (mol/s) | 197 | 197 | 197 |

with main column. The main column has 10 stages (including reboiler and condenser) with the 3rd to 5th constituting the reactive zone, while the side column has 3 stages, all reactive.

### *4.6. Dynamic analysis and operational optimization with explicit model predictive control*

In this step, we take the above derived reactive distillations systems to dynamic analysis, design, and control optimization. Simultaneous design and control will be achieved to close the loop for the proposed framework to ensure economical and smooth operation despite the influence of uncertainty and disturbances.

#### *4.6.1. High fidelity dynamic modeling*

High fidelity dynamic models for the above three MTBE reactive distillation processes (Fig. 10) are developed in gPROMS ModelBuilder®. The basis of the general reactive distillation model has been presented and validated in Schenk et al. (1999) and Georgiadis et al., 2002, which consists of a system of differential and algebraic equations (DAE) for the description of component molar and energy balances for each tray, the partial reboiler and the total condenser, reaction kinetics, phase equilibrium, etc.

The major design and operating parameters of the three reactive distillation systems for dynamic modeling and simulation are given in Table 6. Note that since rate-based reaction kinetic calculation is utilized in the high fidelity dynamic models to reflect the actual kinetic-controlled characteristics in MTBE reactive distillation, more column trays are reported in Table 6 comparing to the design results obtained from Aspen Plus® assuming physical and chemical equilibrium (Table 5).

#### *4.6.2. Open-loop analysis with operability and safety considerations*

In this step, we perform open-loop analysis to check if the derived dynamic RD systems are sustaining their desired level of operability and safety as promised by steady-state design (Section 4.4).

The model-based risk assessment approach introduced in Section 3.4 is also incorporated in dynamic modeling and simulation to calculate process risk values as “inherent safety indicators”. Since the risk reduction is specified on a comparative basis, for simplicity we define a scaled measurement value as “Risk Ratio”. As a base case, the Nominal Design has a Risk Ratio of 1. Thereby the Risk Ratios of Operable Design 1 and 2 are expected to be around 0.8 for consistency with the inherent safety promises given by steady-state synthesis with safety considerations (i.e., reducing at least 20% of process risk). The actual Risk Ratios calculated from dynamic simulation are 0.91 and 0.81 respectively for Operable Design 1 and 2. Both of the designs are inherent safer with respect to Nominal Design, although Design 1 not fully achieving the desired inherent safety level. However, since the identification and translation of equipment-based steady-state/dynamic RD designs from phenomena-based synthesis are based on “trial-and-error” attempts, we will later incorporate risk calculation in dynamic optimization to maintain process risks at the desired level.

Regarding flexibility considerations, steady-state Nominal Design is not flexible over the uncertainty range of methanol feed flowrate (i.e. 205.5 mol/s - 225.5 mol/s), while Design 1 and 2 are derived based on the flexibility test. To check the flexibility at this dynamic stage, the feasible regions of the three reactive distillation systems are depicted in Figs. 11. In addition to the uncertainty range, the above RD systems are also analyzed with respect to a disturbance in the IB4 inlet composition, which will be introduced later for control investigations. As can be seen, Nominal Design cannot operate over the entire range of uncertainty or disturbances while Operable Design 1 and 2 do provide much better operability performance, which is consistent with the results obtained via steady-state operability analysis.

#### *4.6.3. Multi-Parametric model predictive control and closed-loop validation*

Since Nominal Design has been proved to be not operable in presence of uncertainty and disturbances, the following control analysis will only consider Operable Design 1 and 2.

In both of these two RD systems, the butenes feed flowrate is utilized as a manipulated variable and the MTBE molar composition in the bottom product is treated as the control variable with a desired set point of 98%. The other process specification on MTBE product flowrate, previously defined for steady-state synthesis, is assumed to be satisfied with perfect flow control. Thus the MTBE reactive distillation columns are single input single output (SISO) systems.

The mp-MPC controllers are designed following the PAROC framework (Pistikopoulos et al., 2015). A linear state-space approximated model is first derived for each RD design to reduce complexity of the original high fidelity model while preserving desired level of model accuracy. The System Identification toolbox in MATLAB® is used for this purpose. The mp-MPC control strategy in the form of Eq. 13 is solved with multi-parametric programming techniques provided in the POP® toolbox in MATLAB® to acquire a map of optimal control actions in the form of Eq. (14).

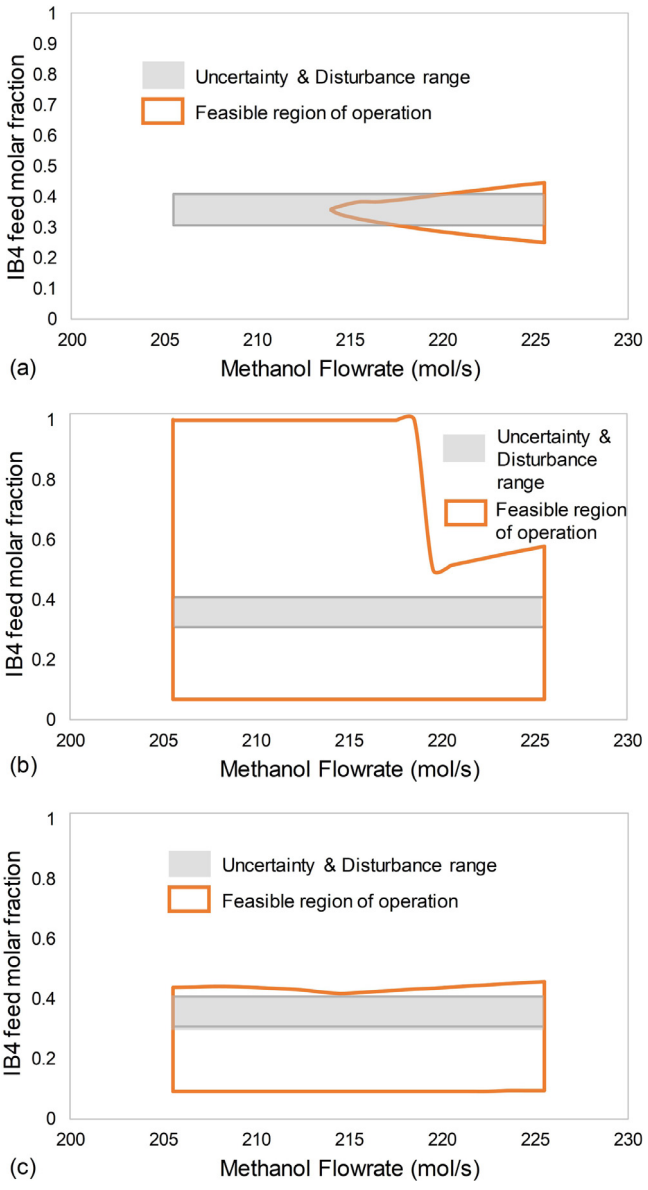


**Fig. 11.** Feasible operation region for MTBE production.
(a) Nominal Design, (b) Operable Design 1, (c) Operable Design 2.

It is worth noting that design variables are also aware by the optimal mp-MPC controller as uncertain parameters. In the RD case, we consider column diameter and catalyst load per tray as continuous design variables, as well as the number of column trays and feed tray locations as discrete ones to be further optimized.

The tuning parameters for the mp-MPC controllers of Operable Design 1 and 2 are presented in Table 7. The closed-loop performance of the above derived mp-MPC controllers against the original high fidelity model is validated as shown in Figs. 12, 13, 14.

*4.6.4. Simultaneous design & control optimization*

To finally close the loop for the synthesis of operable MTBE production systems, simultaneous design and control of Operable Design 1 and 2 are achieved by integrating the rigorous process model and design-dependent mp-MPC controllers via mixed-integer dynamic optimization. The optimization objective is to minimize total annual cost as given in Eq. 19, where a payback period of three years is used. The mp-MPC integrated dynamic optimization results are summarized in Table 8. Also note that the risk ratio of both designs are kept under 80% of the Nominal

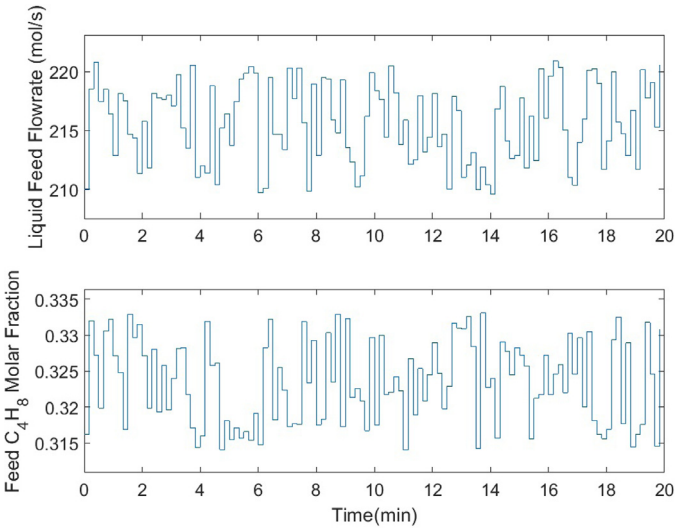


**Fig. 12.** Disturbance profile for closed loop validation.

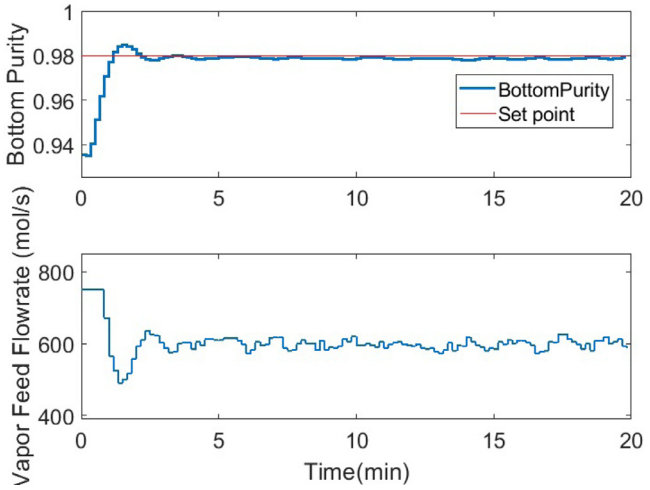


**Fig. 13.** Closed loop validation for Operable Design 1.

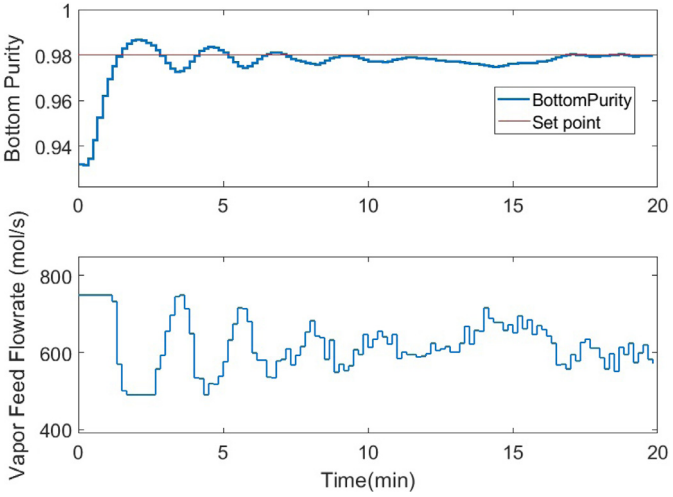


**Fig. 14.** Closed loop validation for Operable Design 2.

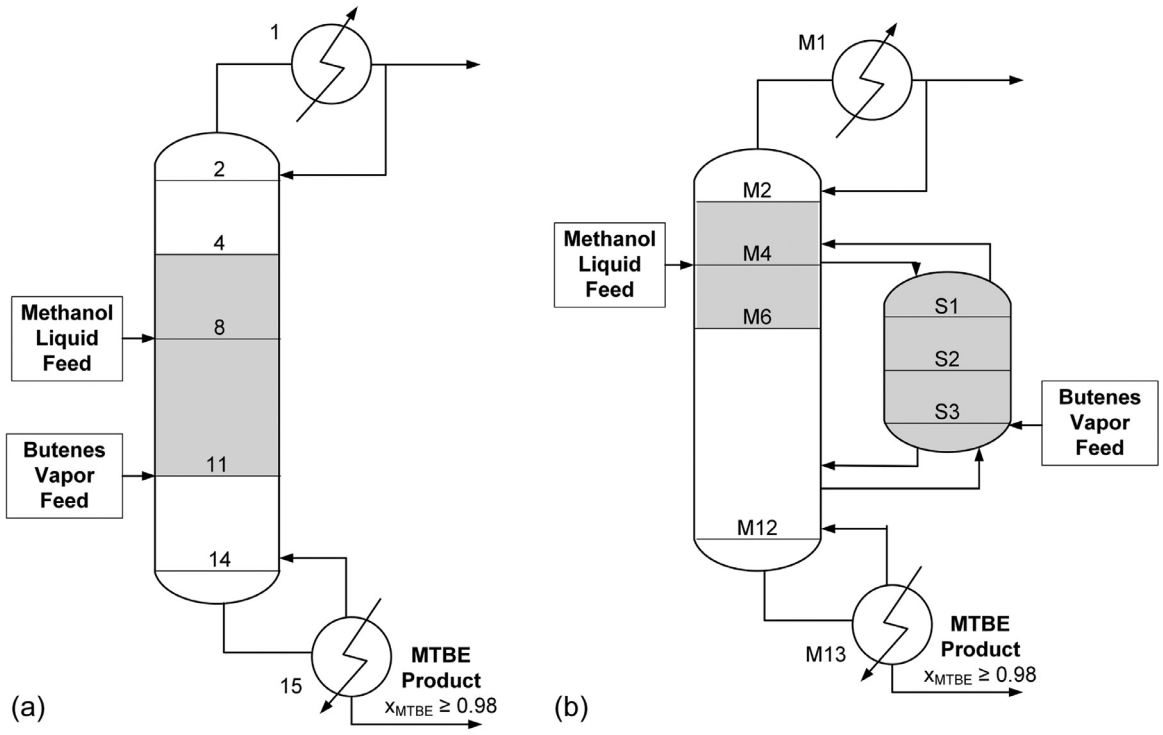


**Fig. 15.** Operable intensified reactive distillation systems for MTBE production.
(a) Design 1, (b) Design 2.
Shaded trays: reactive zone, M: main column, S: side column.

**Table 7**
Tuning parameters for design-dependent mp-MPC of Operable Design 1 and 2.

| MPC design parameters | Design 1 | Design 2 |
|---|---|---|
| $OH$ | 2 | 4 |
| $CH$ | 1 | 3 |
| $QR$ | $5E6$ | $1E5$ |
| $R$ | $1E5$ | $1E5$ |
| $u_{min}$ | 490 | 490 |
| $u_{max}$ | 750 | 750 |
| $y_{min}$ | $[0\ 0]^T$ | $[0\ 0]^T$ |
| $y_{max}$ | $[1\ 1600]^T$ | $[1\ 1600]^T$ |
| $d_{min}$ | $[205.5\ 0.3]^T$ | $[205.5\ 0.3]^T$ |
| $d_{max}$ | $[235.5\ 0.4078]^T$ | $[235.5\ 0.4078]^T$ |

**Table 8**
MTBE production – Simultaneous design & control optimization.

| | Design 1 | Design 2 |
|---|---|---|
| Column diameter (m) | 2.0 | 2.3 |
| Number of trays | 13 | 9 (main)<br>3 (side) |
| Feed tray location 1 | 10 | 3 (side) |
| Feed tray location 2 | 7 | 3 (main) |
| Catalyst mass (ton) | 4.4 | 6.5 |
| Column cost ($\times 10^6$\$/$yr$) | 0.042 | 0.090 |
| Catalyst cost ($\times 10^6$\$/$yr$) | 0.076 | 0.113 |
| Operating cost ($\times 10^6$\$/$yr$) | 2.290 | 3.397 |
| Total cost ($\times 10^6$\$/$yr$) | 2.408 | 3.601 |
| Risk ratio | 0.79 | 0.78 |

Design, thus consistent with the steady-state synthesis operability and safety promises.

### *4.7. Verifiable and operable intensified designs for MTBE production*

Up to this stage, two designs (Fig. 15) have been obtained for the MTBE production task under consideration. The trade-offs between their cost, operability, safety, and control performances have been thoroughly investigated and can be used to assist further decision making, as shown in Table 8.

## 5. Conclusion

In this work, we have proposed a framework for the synthesis of operable process intensification systems, leveraging: (i) phenomena-based GMF synthesis representation strategy to generate novel intensified process solutions, (ii) flexibility analysis to accommodate process uncertainty, (iii) risk assessment to evaluate inherent safety at both steady-state and dynamic conceptual design stage; and (iv) explicit/multi-parametric MPC via the PAROC framework. It has been well demonstrated via the MTBE production case study that the proposed approach can systematically integrate different conceptual design tasks and consistently lead to the design of verifiable, intensified, and operable reactive separation systems. Ongoing work focuses on the extension of the proposed framework to explore the role of (advanced) materials in process intensification, taking extractive separation as an example.

## Declaration of Competing Interest

The authors declare that they have no known competing financial interests or personal relationships that could have appeared to influence the work reported in this paper.

## CRediT authorship contribution statement

**Yuhe Tian:** Methodology, Software, Validation, Formal analysis, Writing - original draft. **Iosif Pappas:** Software, Validation, Formal analysis, Writing - review & editing. **Baris Burnak:** Validation, Formal analysis, Writing - review & editing. **Justin Katz:** Validation, Formal analysis, Writing - review, and editing. **Efstratios N. Pistikopoulos:** Conceptualization, Supervision, Project administration, Funding acquisition.

## Acknowledgement

Financial support from the Texas A&M Energy Institute, Shell, NSF PAROC Project (Grant No. 1705423), and RAPID SYNOPSIS Project (DE-EE0007888-09-03) is gratefully acknowledged.

## References

Al-Arfaj, M.A., Luyben, W.L., 2002. Comparative control study of ideal and methyl acetate reactive distillation. Chem. Eng. Sci. 57 (24), 5039–5050.
Al-Arfaj, M.A., Luyben, W.L., 2002. Design and control of an olefin metathesis reactive distillation column. Chem. Eng. Sci. 57 (5), 715–733.
Algusane, T.Y., Proios, P., Georgiadis, M.C., Pistikopoulos, E.N., 2006. A framework for the synthesis of reactive absorption columns. Chem. Eng. Process. 45 (4), 276–290.
Avraamidou, S., Baratsas, S.G., Tian, Y., Pistikopoulos, E.N., 2020. Circular economy – a challenge and an opportunity for process systems engineering. Comput. Chem. Eng. 133, 106629.
Babi, D.K., Cruz, M.S., Gani, R., 2016. Fundamentals of process intensification: a process systems engineering view. In: Process Intensification in Chemical Engineering. Springer, pp. 7–33.
Babi, D.K., Holtbruegge, J., Lutze, P., Gorak, A., Woodley, J.M., Gani, R., 2015. Sustainable process synthesis-intensification. Comput. Chem. Eng. 81, 218–244.
Baldea, M., 2015. From process integration to process intensification. Comput. Chem. Eng. 81, 104–114.
Baldea, M., Edgar, T.F., Stanley, B.L., Kiss, A.A., 2017. Modular manufacturing processes: status, challenges, and opportunities. AIChE J. 63 (10), 4262–4272.
Baldea, M., Hasan, M.M.F., Boukouvala, F., 2019. (Eds.). frameworks for process intensification and modularization. [Special Issue]. Ind. Eng. Chem. Res. 58 (15).
Bemporad, A., Morari, M., Dua, V., Pistikopoulos, E.N., 2002. The explicit linear quadratic regulator for constrained systems. Automatica 38 (1), 3–20.
Bhosekar, A., Ierapetritou, M., 2018. Advances in surrogate based modeling, feasibility analysis, and optimization: a review. Comput. Chem. Eng. 108, 250–267.
Bielenberg, J., Fletcher, K., El-Halwagi, M., Ng, K.M., 2018. (Eds.). process systems engineering: process intensification. [Special Issue]. Current Opin. Chem. Eng. 22.
Bielenberg, J., Palou-Rivera, I., 2019. The RAPID manufacturing institute – Reenergizing us efforts in process intensification and modular chemical processing. Chem. Eng. Process. https://doi.org/10.1016/j.cep.2019.02.008.
BP plc, 2019. BP energy outlook 2019, Visited 15 August 2019. https://www.bp.com/en/global/corporate/energy-economics/energy-outlook.html.
Burnak, B., Diangelakis, N.A., Pistikopoulos, E.N., 2019. Towards the grand unification of process design, scheduling, and control – utopia or reality? Processes 7 (7), 461.
Burri, J.F., Wilson, S.D., Manousiouthakis, V.I., 2002. Infinite dimensional state-space approach to reactor network synthesis: application to attainable region construction. Comput. Chem. Eng. 26 (6), 849–862.
Carrasco, J.C., Lima, F.V., 2017. Novel operability-based approach for process design and intensification: application to a membrane reactor for direct methane aromatization. AIChE J. 63 (3), 975–983.
Castillo-Landero, A., Ortiz-Espinoza, A.P., Jimenez-Gutierrez, A., 2018. A process intensification methodology including economic, sustainability, and safety considerations. Ind. Eng. Chem. Res. 58 (15), 6080–6092.
Charpentier, J.C., 2007. In the frame of globalization and sustainability, process intensification, a path to the future of chemical and process engineering (molecules into money). Chem. Eng. J. 134 (1–3), 84–92.
Chen, B., Westerberg, A.W., 1986. Structural flexibility for heat integrated distillation columns i. analysis. Chem. Eng. Sci. 41 (2), 355–363.
Colombo, F., Cori, L., Dalloro, L., Delogu, P., 1983. Equilibrium constant for the methyl tert-butyl ether liquid-phase synthesis using UNIFAC. Ind. Eng. Chem. Fundament. 22 (2), 219–223.
da Cruz, F.E., Manousiouthakis, V.I., 2019. Process intensification of multipressure reactive distillation networks using infinite dimensional state-space (IDEAS). Ind. Eng. Chem. Res. 58 (15), 5968–5983.
Demirel, S.E., Li, J., Hasan, M.F., 2017. Systematic process intensification using building blocks. Comput. Chem. Eng. 105, 2–38.
Demirel, S.E., Li, J., Hasan, M.F., 2019. A general framework for process synthesis, integration, and intensification. Ind. Eng. Chem. Res. 58 (15), 5950–5967.
Demirel, S.E., Li, J., Hasan, M.F., 2019. Systematic process intensification. Curr. Opin. Chem. Eng. https://doi.org/10.1016/j.coche.2018.12.001.
Demirhan, C.D., Tso, W.W., Ogumerem, G.S., Pistikopoulos, E.N., 2019. Energy systems engineering – a guided tour. BMC Chem. Eng. 1 (1), 11.
Diangelakis, N.A., Burnak, B., Katz, J., Pistikopoulos, E.N., 2017. Process design and control optimization: a simultaneous approach by multi-parametric programming. AIChE J. 63 (11), 4827–4846.
Dias, L.S., Ierapetritou, M.G., 2019. Optimal operation and control of intensified processes – Challenges and opportunities. Curr. Opin. Chem. Eng. https://doi.org/10.1016/j.coche.2018.12.008.
Etchells, J., 2005. Process intensification: safety pros and cons. Process Saf. Environ. Protect. 83 (2), 85–89.
Feinberg, M., Ellison, P., 2001. General kinetic bounds on productivity and selectivity in reactor-separator systems of arbitrary design: principles. Ind. Eng. Chem. Res. 40 (14), 3181–3194.
Flemish Government, 2009. Handbook failure frequencies 2009 for drawing up a safety report.
Floudas, C.A., 1995. Nonlinear and mixed-integer optimization: fundamentals and applications. Oxford University Press.
Freeman, R.A., 1989. CCPS Guidelines for chemical process quantitative risk analysis. Plant/Oper. Progr.
Freund, H., Sundmacher, K., 2008. Towards a methodology for the systematic analysis and design of efficient chemical processes: part 1. from unit operations to elementary process functions. Chem. Eng. Process. 47 (12), 2051–2060.
Frumkin, J.A., Doherty, M.F., 2018. Target bounds on reaction selectivity via feinberg's CFSTR equivalence principle. AIChE J. 64 (3), 926–939.
Garg, N., Woodley, J.M., Gani, R., Kontogeorgis, G.M., 2019. Sustainable solutions by integrating process synthesis-intensification. Comput. Chem. Eng. 126, 499–519.
Gazzaneo, V., Lima, F.V., 2019. Multilayer operability framework for process design, intensification, and modularization of nonlinear energy systems. Ind. Eng. Chem. Res. 58 (15), 6069–6079.
Georgiadis, M.C., Schenk, M., Pistikopoulos, E.N., Gani, R., 2002. The interactions of design control and operability in reactive distillation systems. Comput. Chem. Eng. 26 (4–5), 735–746.
Grossmann, I.E., Floudas, C.A., 1987. Active constraint strategy for flexibility analysis in chemical processes. Comput. Chem. Eng. 11 (6), 675–693.
Halemane, K.P., Grossmann, I.E., 1983. Optimal process design under uncertainty. AIChE J. 29 (3), 425–433.
Harmsen, G.J., 2007. Reactive distillation: the front-runner of industrial process intensification: a full review of commercial applications, research, scale-up, design and operation. Chem. Eng. Process. 46 (9), 774–780.
Intergovernmental Panel on Climate Change, 2014. AR5 synthesis report: Climate change 2014, Visited 15 August 2019. https://www.ipcc.ch/report/ar5.
International Energy Agency, 2018. World energy outlook 2018, Visited 9 October 2019. https://www.iea.org/weo2018.
Ismail, S.R., Pistikopoulos, E.N., Papalexandri, K.P., 1999. Modular representation synthesis framework for homogeneous azeotropic separation. AIChE J. 45 (8), 1701–1720.
Ismail, S.R., Pistikopoulos, E.N., Papalexandri, K.P., 1999. Synthesis of reactive and combined reactor/separation systems utilizing a mass/heat exchange transfer module. Chem. Eng. Sci. 54 (13–14), 2721–2729.
Ismail, S.R., Proios, P., Pistikopoulos, E.N., 2001. Modular synthesis framework for combined separation/reaction systems. AIChE J. 47 (3), 629–649.
Kaiser, N.M., Flassig, R.J., Sundmacher, K., 2016. Probabilistic reactor design in the framework of elementary process functions. Comput. Chem. Eng. 94, 45–59.
Kaiser, N.M., Flassig, R.J., Sundmacher, K., 2018. Reactor-network synthesis via flux profile analysis. Chem. Eng. J. 335, 1018–1030.
Kalakul, S., Zhang, L., Choudhury, H.A., Elbashir, N.O., Eden, M.R., Gani, R., 2018. ProCAPD – A computer-aided model-based tool for chemical product design and analysis. In: Computer Aided Chemical Engineering, 44. Elsevier, pp. 469–474.
Keil, F.J., 2018. Process intensification. Rev. Chem. Eng. 34 (2), 135–200.
Khajuria, H., Pistikopoulos, E.N., 2013. Optimization and control of pressure swing adsorption processes under uncertainty. AIChE J. 59 (1), 120–131.
Kiss, A.A., Jobson, M., Gao, X., 2018. Reactive distillation: stepping up to the next level of process intensification. Ind. Eng. Chem. Res. 58 (15), 5909–5918.
Kiss, A.A., Rewagad, R.R., 2011. Energy efficient control of a BTX dividing-wall column. Comput. Chem. Eng. 35 (12), 2896–2904.
Kuhlmann, H., Skiborowski, M., 2017. Optimization-based approach to process synthesis for process intensification: general approach and application to ethanol dehydration. Ind. Eng. Chem. Res. 56 (45), 13461–13481.
Kuhlmann, H., Veith, H., Mooller, M., Nguyen, K.-P., Gorak, A., Skiborowski, M., 2017. Optimization-based approach to process synthesis for process intensification: synthesis of reaction-separation processes. Ind. Eng. Chem. Res. 57 (10), 3639–3655.
Li, J., Demirel, S.E., Hasan, M.F., 2018. Process integration using block superstructure. Ind. Eng. Chem. Res. 57 (12), 4377–4398.
Li, J., Demirel, S.E., Hasan, M.F., 2018. Process synthesis using block superstructure with automated flowsheet generation and optimization. AIChE J. 64 (8), 3082–3100.
Liesche, G., Schack, D., Sundmacher, K., 2019. The fluxmax approach for simultaneous process synthesis and heat integration: production of hydrogen cyanide. AIChE J. e16554.
Lin, C.-T., 1974. Structural controllability. IEEE Trans. Automat. Control 19 (3), 201–208.
Ling, H., Luyben, W.L., 2009. New control structure for divided-wall columns. Ind. Eng. Chem. Res. 48 (13), 6034–6049.
Ling, H., Luyben, W.L., 2009. Temperature control of the btx divided-wall column. Ind. Eng. Chem. Res. 49 (1), 189–203.
Lopez-Arenas, T., Sales-Cruz, M., Gani, R., Pérez-Cisneros, E.S., 2019. Thermodynamic analysis of the driving force approach: reactive systems. Comput. Chem. Eng. 129, 106509.
Lutze, P., Babi, D.K., Woodley, J.M., Gani, R., 2013. Phenomena based methodology for process synthesis incorporating process intensification. Ind. Eng. Chem. Res. 52 (22), 7127–7144.
Lutze, P., Gani, R., Woodley, J.M., 2010. Process intensification: a perspective on process synthesis. Chem. Eng. Process. 49 (6), 547–558.
Luyben, W.L., 2008. Comparison of extractive distillation and pressure-swing distillation for acetone- methanol separation. Ind. Eng. Chem. Res. 47 (8), 2696–2707.

Luyben, W.L., 2008. Effect of solvent on controllability in extractive distillation. Ind. Eng. Chem. Res. 47 (13), 4425–4439.
Mansouri, S.S., Huusom, J.K., Gani, R., Sales-Cruz, M., 2016. Systematic integrated process design and control of binary element reactive distillation processes. AIChE J. 62 (9), 3137–3154.
Mansouri, S.S., Sales-Cruz, M., Huusom, J.K., Gani, R., 2016. Systematic integrated process design and control of reactive distillation processes involving multi-elements. Chem. Eng. Res. Des. 115, 348–364.
Margot, F., 2010. Symmetry in integer linear programming. In: 50 Years of Integer Programming 1958–2008. Springer, pp. 647–686.
Medina-Herrera, N., Grossmann, I.E., Mannan, M.S., Jimenez-Gutierrez, A., 2014. An approach for solvent selection in extractive distillation systems including safety considerations. Ind. Eng. Chem. Res. 53 (30), 12023–12031.
Moulijn, J.A., Stankiewicz, A., Grievink, J., Gorak, A., 2006. Process intensification and process system engineering: A friendly symbiosis. In: Computer Aided Chemical Engineering, 21. Elsevier, pp. 29–37.
Nemet, A., Klemeš, J.J., Kravanja, Z., 2018. Process synthesis with simultaneous consideration of inherent safety-inherent risk footprint. Front. Chem. Sci. Eng. 12 (4), 745–762.
Nemet, A., Klemeš, J.J., Moon, I., Kravanja, Z., 2017. Safety analysis embedded in heat exchanger network synthesis. Comput. Chem. Eng. 107, 357–380.
Nikačević, N.M., Huesman, A.E., Van den Hof, P.M., Stankiewicz, A.I., 2012. Opportunities and challenges for process control in process intensification. Chem. Eng. Process. 52, 1–15.
Oberdieck, R., Diangelakis, N.A., Papathanasiou, M.M., Nascu, I., Pistikopoulos, E.N., 2016. POP – Parametric optimization toolbox. Ind. Eng. Chem. Res. 55 (33), 8979–8991.
Panjwani, P., Schenk, M., Georgiadis, M., Pistikopoulos, E., 2005. Optimal design and control of a reactive distillation system. Eng. Opt. 37 (7), 733–753.
Papalexandri, K., Pistikopoulos, E.N., 1994. A multiperiod minlp model for the synthesis of flexible heat and mass exchange networks. Comput. Chem. Eng. 18 (11–12), 1125–1139.
Papalexandri, K.P., Pistikopoulos, E.N., 1996. Generalized modular representation framework for process synthesis. AIChE J. 42 (4), 1010–1032.
Papathanasiou, M.M., Burnak, B., Katz, J., Shah, N., Pistikopoulos, E.N., 2019. Assisting continuous biomanufacturing through advanced control in downstream purification. Comput. Chem. Eng. 125, 232–248.
Pichardo, P., Manousiouthakis, V.I., 2017. Infinite dimensional state-space as a systematic process intensification tool: energetic intensification of hydrogen production. Chem. Eng. Res. Des. 120, 372–395.
Pistikopoulos, E.N., Diangelakis, N.A., Oberdieck, R., Papathanasiou, M.M., Nascu, I., Sun, M., 2015. PAROC – An integrated framework and software platform for the optimisation and advanced model-based control of process systems. Chem. Eng. Sci. 136, 115–138.
Proios, P., 2004. Generalized modular framework for distillation column synthesis. Imperial College London (University of London).
Proios, P., Goula, N.F., Pistikopoulos, E.N., 2005. Generalized modular framework for the synthesis of heat integrated distillation column sequences. Chem. Eng. Sci. 60 (17), 4678–4701.
Proios, P., Pistikopoulos, E.N., 2006. Hybrid generalized modular/collocation framework for distillation column synthesis. AIChE J. 52 (3), 1038–1056.
Rehfinger, A., Hoffmann, U., 1990. Kinetics of methyl tertiary butyl ether liquid phase synthesis catalyzed by ion exchange resin – i. intrinsic rate expression in liquid phase activities. Chem. Eng. Sci. 45 (6), 1605–1617 .
Rewagad, R.R., Kiss, A.A., 2012. Dynamic optimization of a dividing-wall column using model predictive control. Chem. Eng. Sci. 68 (1), 132–142.
Roy, N., Eljack, F., Jiménez-Gutiérrez, A., Zhang, B., Thiruvenkataswamy, P., El-Halwagi, M., Mannan, M.S., 2016. A review of safety indices for process design. Curr. Opin. Chem. Eng. 14, 42–48.
Schenk, M., Gani, R., Bogle, D., Pistikopoulos, E., 1999. A hybrid modelling approach for separation systems involving distillation. Chem. Eng. Res. Des. 77 (6), 519–534.
Sitter, S., Chen, Q., Grossmann, I.E., 2019. An overview of process intensification methods. Curr. Opin. Chem. Eng. https://doi.org/10.1016/j.coche.2018.12.006.
Stankiewicz, A.I., Moulijn, J.A., 2000. Process intensification: transforming chemical engineering. Chem. Eng. Progress 96 (1), 22–34.
Stoffen, P.G., 2005. Guidelines for quantitative risk assessment. Ministerie van Volkshuisvesting Ruimtelijke Ordening en Milieu. CPR E 18.
Tian, Y., Demirel, S.E., Hasan, M.F., Pistikopoulos, E.N., 2018. An overview of process systems engineering approaches for process intensification: state of the art. Chem. Eng. Process. 133, 160–210.
Tian, Y., Mannan, M.S., Kravanja, Z., Pistikopoulos, E.N., 2018. Towards the synthesis of modular process intensification systems with safety and operability considerations-application to heat exchanger network. In: Computer Aided Chemical Engineering, 43. Elsevier, pp. 705–710.
Tian, Y., Mannan, M.S., Pistikopoulos, E.N., 2018. Towards a systematic framework for the synthesis of operable process intensification systems. In: Computer Aided Chemical Engineering, 44. Elsevier, pp. 2383–2388.
Tian, Y., Pistikopoulos, E.N., 2018. Synthesis of operable process intensification systems steady-state design with safety and operability considerations. Ind. Eng. Chem. Res. 58 (15), 6049–6068.
Tian, Y., Pistikopoulos, E.N., 2019. Generalized modular representation framework for the synthesis of extractive separation systems. In: Computer Aided Chemical Engineering, 47. Elsevier, pp. 475–480.
Tian, Y., Pistikopoulos, E.N., 2019. Synthesis of operable process intensification systems: advances and challenges. Curr. Opin. Chem. Eng 25, 101–107.
Tula, A.K., Babi, D.K., Bottlaender, J., Eden, M.R., Gani, R., 2017. A computer-aided software-tool for sustainable process synthesis-intensification. Comput. Chem. Eng. 105, 74–95.
Tula, A.K., Eden, M.R., Gani, R., 2019. Computer-aided process intensification: Challenges, trends and opportunities. AIChE Journal. https://doi.org/10.1002/aic.16819.
U.S. Energy Information Administration, 2019. Annual energy outlook 2019 with projections to 2050, Visited 9 October 2019. https://www.eia.gov/outlooks/aeo/pdf/aeo2019.pdf.
Westerberg, A.W., Chen, B., 1986. Structural flexibility for heat integrated distillation columns II. synthesis. Chem. Eng. Sci. 41 (2), 365–377.
Wilhite, B., Ierapetritou, M., 2019. (Eds.). process intensification in the united states: recent developments, emerging opportunities and perspectives. [Special Issue]. Chem. Eng. Process.
Yuan, Z., Chen, B., Sin, G., Gani, R., 2012. State-of-the-art and progress in the optimization-based simultaneous design and control for chemical processes. AIChE J. 58 (6), 1640–1659.
Zhou, W., Manousiouthakis, V.I., 2006. Non-ideal reactor network synthesis through ideas: attainable region construction. Chem. Eng. Sci. 61 (21), 6936–6945.